



**Lehrstuhl für
Technische Dynamik**
Prof. Dr.-Ing. habil. Sigrid Leyendecker

Report

Institute of Applied Dynamics

2020



**FRIEDRICH-ALEXANDER
UNIVERSITÄT
ERLANGEN-NÜRNBERG**
TECHNISCHE FAKULTÄT

© 2020

Prof. Dr.-Ing. habil. S. Leyendecker
Lehrstuhl für Technische Dynamik
Friedrich-Alexander-Universität Erlangen-Nürnberg
Immerwahrstrasse 1
91058 Erlangen
Tel.: 09131 8561000
Fax.: 09131 8561011
www: <https://www.ltd.tf.fau.de>

Editors: E. Fleischmann, D. Phansalkar

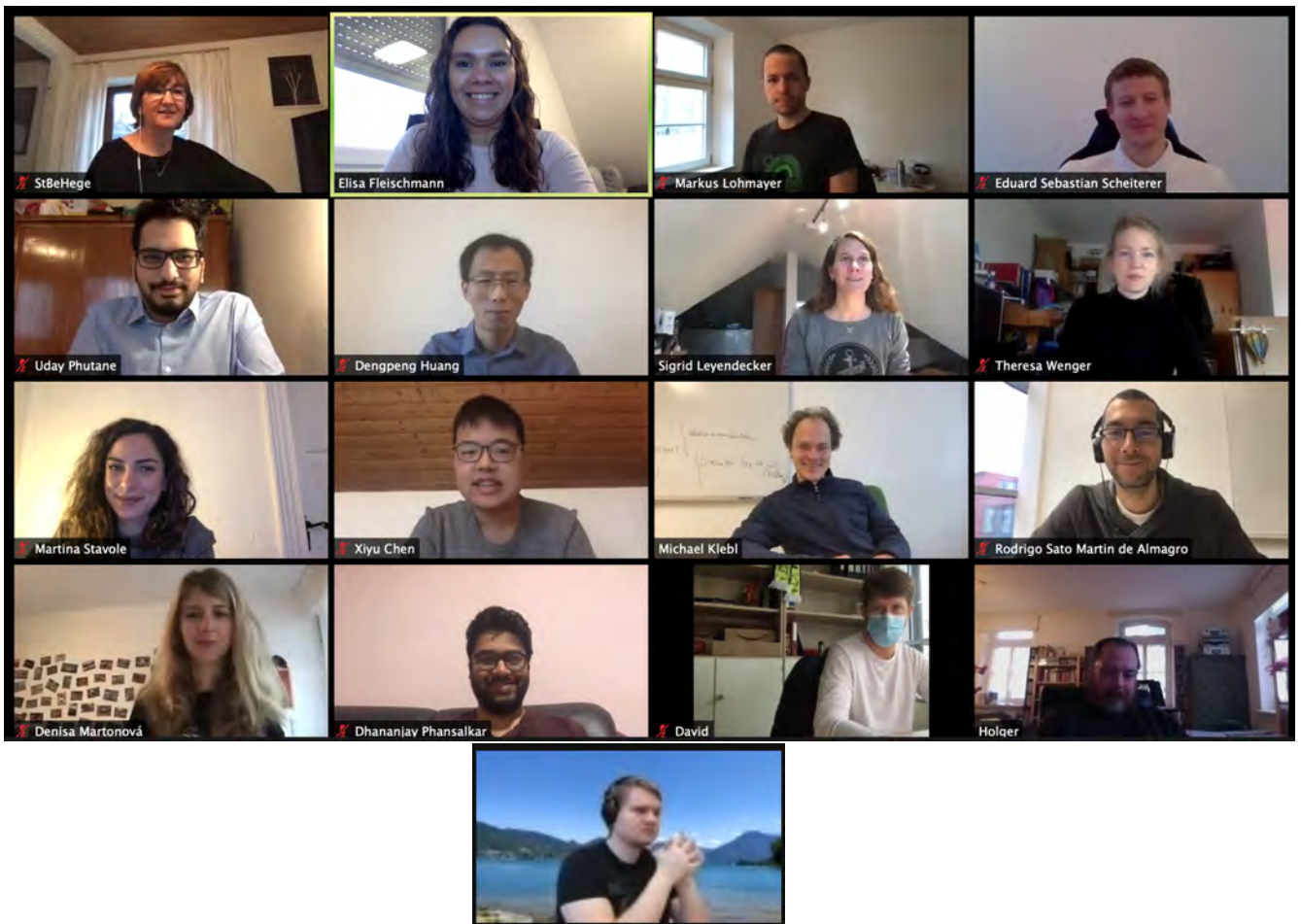
All rights reserved. Without explicit permission of the authors it is not allowed to copy this publication or parts of it, neither by photocopy nor in electronic media.

Contents

1	Preface	4
2	Team	5
3	Research	7
3.1	ETN – THREAD	7
3.2	FRASCAL – Fracture across Scales	7
3.3	SPP 1886	7
3.4	DFG dielectric elastomer project	7
3.5	Heart project	8
3.6	Characterisation of Macromolecules	8
3.7	BMBF 05M2016 – DYMARA	8
3.8	Scientific reports	8
4	Activities	32
4.1	Teaching during Covid-19 pandemic	32
4.2	Motion capture laboratory	33
4.3	Dynamic laboratory	34
4.4	MATLAB laboratory	35
4.5	Summer school: Fundamentals of beam theory and flexible multibody dynamics	35
4.6	Teaching	37
4.7	Theses	39
4.8	Seminar for mechanics	39
4.9	Editorial activities	39
5	Publications	41
5.1	Reviewed journal publications	41
5.2	Invited lectures	41
5.3	Conferences and proceedings	41
6	Social events	42

1 Preface

This report gives a summary of the scientific and teaching activities of the Institute of Applied Dynamics (LTD) at the Friedrich-Alexander-Universität Erlangen-Nürnberg during the year 2020. The members of LTD are passionately working on topics such as multibody dynamics and robotics, motion capturing, biomechanics, structure preserving methods and optimal control. Many thanks to our technical, scientific and admin staff at LTD and also to all the students involved to make it a successful year at the Institute of Applied Dynamics. We wish you an enjoyable time glancing through our annual report.



2 Team

institute holder

Prof. Dr.-Ing. habil. Sigrid Leyendecker

technical staff

Beate Hegen
M.Sc. Elisa Fleischmann
M.Sc. Markus Lohmayer

academic scientist

Dr. rer. nat. Holger Lang

postdoc

Dr. Rodrigo Sato Martín de Almagro

scientific staff

M.Sc.hons. Xiyu Chen
M.Sc. David Holz
M.Sc. Dengpeng Huang
M.Sc. Michael Klebl
M.Sc. Denisa Martonová
M.Sc. Johann Penner
M.Sc. Dhananjay Phansalkar
M.Sc. Uday Phutane
M.Sc. Eduard Sebastian Scheiterer
M.Sc. Martina Stavoletto
M.Sc. Theresa Wenger

from 01.05.2020

students

Johannes Bayer	Niko Beck	Anja Boebel
Dorothea Brackenhauer	Johanna Brosel	Patrick Deferner
Marc Gadiner	Carla Gerlach	Christian Gmeiner
Alexander Greiner	Maximilian Hausch	Simon Heinrich
Daphne Hohbohm	Xuyue Huang	Anne Kirsch
Ogulhan Kizilkaya	Lea Köstler	Deepakraj Krishna Kunder
Xihao Liu	Tanya Neeraj	Carmen Neubauer
Nivashini Radhakrishnan	Julian Reiner	Matthias Schubert
Kristin Schuh	Nicolas Valbuena	Quirin von Rekowski
Felix Werner	Pauline Wittermann	Fabian Wonn
Annalena Wrobel	Juliane Wunder	

Student assistants are mainly active as tutors for young students in basic and advanced lectures at the Bachelor and Master level. Their contribution to high quality teaching is indispensable, thus financial support from various funding sources is gratefully acknowledged.



B. Hegen



E. Fleischmann



M. Lohmayer



H. Lang



X. Chen



D. Holz



D. Huang



M. Klebl



D. Martonová



J. Penner



D. Phansalkar



U. Phutane



R.T. Sato



E.S. Scheiterer



M. Stavole



T. Wenger



S. Leyendecker

3 Research

3.1 ETN – THREAD

The Institute of Applied Dynamics plays an important role in the ETN (European Training Network) project “Joint Training on Numerical Modelling of Highly Flexible Structures for Industrial Applications – THREAD” funded by the European Commission's Marie Skłodowska Curie Programme which is part of Horizon 2020. The project is coordinated by Prof. Dr. Martin Arnold from the Institute of Mathematics at the Martin Luther University Halle-Wittenberg (MLU), Prof. Dr.-Ing. habil. Sigrid Leyendecker is principal investigator and work package leader (geometric numerical methods for rod system dynamics) and M.Sc. Martina Stavole joined the programme as ESR early this year.

THREAD addresses the mechanical modelling, mathematical formulations and numerical methods for highly flexible slender structures like yarns, cables, hoses or ropes that are essential parts of high-performance engineering systems. The complex response of such structures in real operational conditions is far beyond the capabilities of current virtual prototyping tools.

The project had a successful first annual meeting on 19-22 October 2020 in Kaiserslautern, Germany with online access via video conference.

3.2 FRASCAL – Fracture across Scales

The DFG research training group FRASCAL – Fracture across Scales (GRK 2423) led by Prof. Dr.-Ing. habil. Paul Steinmann from the Institute of Applied Mechanics at FAU Erlangen-Nürnberg has successfully continued its research goals. The Institute of Applied Dynamics takes part within FRASCAL P9 project – Adaptive Dynamic Fracture Simulation. The project is supervised by Prof. Dr.-Ing. habil. Sigrid Leyendecker and carried out by M.Sc. Dhananjay Phansalkar. It aims to develop robust and efficient numerical techniques to investigate kinetics of fracture mechanics. It will require adaptive strategies to obtain suitable combinations of spatial and temporal mesh. These methods are developed in close cooperation with RTG's Mercator fellow Prof. Dr. Michael Ortiz. The Visitor's workshop took place on March 12th, 2020 in Atzelsberg near Erlangen. It allowed for discussion with experts from various fields. And midway through the project on September 14 and 15, 2020 the members of FRASCAL met at Fraunhofer Research Campus, Waischenfeld for an RTG retreat.

3.3 SPP 1886

The German Research Foundation (DFG) Priority Programme “Polymorphic uncertainty modelling for the numerical design of structures – SPP 1886” is coordinated by Professor Dr.-Ing. Michael Kaliske from Technische Universität Dresden and Prof. Dr.-Ing. habil. Sigrid Leyendecker is part of the programme committee and principal investigator of one of the projects. In 2020, the Institute of Applied Dynamics had successfully took part in the Phase2-Kickoff Meeting in June, as well as in the second Annual Meeting in November, where the progress in the research of dynamic analysis of prosthetic structures with polymorphic uncertainty was presented.

3.4 DFG dielectric elastomer project

The new DFG-Einzelförderung / Sachbeihilfe “Electromechanically coupled beam models for stacked dielectric elastomer actuators” project, initiated this year with Prof. Dr.-Ing. habil. Sigrid Leyendecker as project leader and fellow M.Sc. Dengpeng Huang in the research front. Stacked dielectric elastomer actuators bear analogy to the behaviour of human muscles in terms of contracting in length direction when stimulated. They are suitable for point-by-point application of a force. Therefore, dielectric elastomers allow for a sophisticated, efficient and noiseless actuation of systems. However, the use of elastic actuators is also accompanied by new control challenges. As the computational cost for solving

optimal control problems is significantly affected by the number of model degrees of freedom, reduced and problem specific actuator models are superior to general but cost-intensive finite element models.

3.5 Heart project

The heart project is focusing on the modelling of the cardiac function to better understand cardiovascular disease, to be able to early detect or even predict heart failure and develop adequate patient specific therapies and medical devices. We are currently working on a rat as well as a human heart model. The former is related to the rat heart project, which is an established research cooperation between the Institute of Applied Dynamics and the Pediatric Cardiology at Friedrich-Alexander-Universität Erlangen-Nürnberg and is funded by the Klaus Tschira Stiftung. The goal of the project is to explore the heart function under pathological and normal conditions by developing a computational model of a rat heart which will be validated with experiments at the Pediatric Cardiology. In 2020, we were mainly focusing on the first steps towards the development of a heart support system as well as determination of a desired transmural fibre and sheet distributions in the myocardium.

3.6 Characterisation of Macromolecules

The characterisation of macromolecules project is a cooperation research between the Institute of Applied Dynamics at Friedrich-Alexander-Universität Erlangen-Nürnberg and SLAC National Accelerator Laboratory at Stanford University and is funded by German Research Foundation (DFG). The purpose of this project is characterizing macromolecules e.g. kinases by using the kino-geometric sampling (KGS) method. The rigidity and conformation transition analysis of macromolecules, will benefit drug development in the cancer field. The project is cooperated by Dr. Henry van den Bedem from Stanford University. M.Sc. Xiyu Chen is focusing on the rigidity analysis and the change of entropy binding with ligands by using the KGS method.

3.7 BMBF 05M2016 – DYMARA

The DYMARA project was funded by the Federal Ministry of Education and Research (BMBF) under the funding priority “Healthy Life” and it successfully ended this year. The joint project was coordinated by Prof. Dr. rer. nat. habil. Bernd Simeon from Technische Universität Kaiserslautern (UNIKL) and had a thematic relation to ergonomics and health promotion at work. As part of the collaborative project, Johann Penner at LTD investigated muscle paths in the biomechanical simulation of human motion and the integration of new fiber-based muscle models to multibody dynamics while the UNIKL was developing a continuum mechanical muscle model.

3.8 Scientific reports

The subsequent pages present a brief overview on the current research projects pursued at the Institute of Applied Dynamics. These are partly financed by third-party funding German Research Foundation (DFG), the Klaus Tschira Stiftung, the Federal Ministry of Education and Research (BMBF) the European Training Network (ETN) and in addition by the core support of the university.

Research topics

Vibrational entropy change for binding with ligands based on the kinematic method
Xiyu Chen, Sigrid Leyendecker, Henry van den Bedem

Modelling the characteristic orthotropic tissue structure in the myocardium
David Holz, Minh Tuan Duong, Denisa Martonová, Muhannad Alkassar, Sven Dittrich, Sigrid

Leyendecker

Electromechanically coupled beam models for stacked dielectric elastomer actuators

Dengpeng Huang, Sigrid Leyendecker

Investigation of optical motion capturing for characterizing movement patterns of the hand in rheumatoid arthritis

Michael Klebl, Uday Phutane, Anna-Maria Liphardt, Johann Penner and Sigrid Leyendecker

Discrete mechanics for static Cosserat rods with forcing

Holger Lang, Sigrid Leyendecker, Joachim Linn

First steps towards a cardiac assist device to support a diseased rat heart

Denisa Martonová, Dorothea Brackenhämmer, David Holz, Maximilian Landgraf, Muhannad Alkassar and Sigrid Leyendecker

Musculoskeletal optimal control simulations with a discrete muscle wrapping formulation and improved contact modelling

Johann Penner, Sigrid Leyendecker

Spatially varying regularisation variable in quasi-static phase-field model for brittle fractures

Dhananjay Phansalkar, Michael Ortiz, Kerstin Weinberg, Sigrid Leyendecker

Grasping via kinematically reduced model of the hand

Uday Phutane, Michael Roller, Sigrid Leyendecker

Understanding variational integrators in field theories

Rodrigo T. Sato Martín de Almagro, Sigrid Leyendecker

Forward dynamics simulation of a human leg with a carbon spring prosthetic foot

Eduard S. Scheiterer, Sigrid Leyendecker

Variational integrators used to solve a 1D wave equation

Martina Stavole, Sigrid Leyendecker

Analysis of multirate variational integrators and mixed order variational integrators by Modulated Fourier expansions

Theresa Wenger, Sina Ober-Blöbaum and Sigrid Leyendecker

Vibrational entropy change for binding with ligands based on the kinematic method

Xiyu Chen, Sigrid Leyendecker, Henry van den Bedem^{1 2}

Protein is a series of amino acid in the sequence, the function of protein and binding with other biomolecules is determined by the folded of protein and 3D structure. Study of the energy and entropy change when binding with ligands benefits to understand the affinity of binding and discover the potential drugs.

In this study, we developed a kinematic method to calculate the vibrational entropy. We start from the Kinematic rigidity analysis (KRA)[1, 2], KRA method is an efficient method and fast method to present the rigidified cluster and rigidified dihedral angles of functional molecule. KRA represents molecules as articulated multi-body complexes with dihedral angles as revolute degree of freedom and selected non-covalent interactions such as hydrogen bonds and hydrophobic interaction as holonomic constraints. The sigular value decomposition (SVD) of the constraint Jacobian matrix provide the information for the rigidified dihedral angles. Base on the rigidified dihedral angles, the position Jacobian matrix is derived as

$$\mathbf{J}_{ij} = \frac{\partial \mathbf{x}_i}{\partial \theta_j} = c_{ij} \mathbf{e}_j \times (\mathbf{x}_i - \mathbf{x}_{j-1}) \in \mathbb{R}^{3 \times 1} \quad \text{for } i = 1, \dots, N \text{ and } j = 1, \dots, n \quad (1)$$

Then we build the Hessian matrix of potential energy \mathbf{H}^θ and \mathbf{E}_k^θ kinetic energy for movable dihedral angles in torsional angle system. They are derived from the Hessian matrix of potential energy \mathbf{H}^x in Cartesian system and \mathbf{M} mass matrix.

$$\mathbf{H}^\theta = \mathbf{J}^T \mathbf{H}^x \mathbf{J} \quad \text{and} \quad \mathbf{E}_k^\theta = \mathbf{J}^T \mathbf{M} \mathbf{J} \quad (2)$$

In the vibrational entropy analysis, the eigenvalue problem gives the information for the vibrational mode. The vibrational frequency \mathbf{v} and vibrational amplitude ω is calculated through solving the generalized eigenvalue equation [3].

$$\mathbf{H}^\theta \mathbf{v} = \omega^2 \mathbf{E}_k^\theta \mathbf{v} \quad (3)$$

Then the vibrational entropy of bio-molecule S_{vib} is calculated based on the vibrational frequency \mathbf{v} and it is derived as

$$S_{vib} = T^{-1} \sum_{i=1}^n \left[\frac{h\nu_i}{e^{h\nu_i/k_B T} - 1} - k_B T \ln(1 - e^{-h\nu_i/k_B T}) \right] \quad (4)$$

where T is the temperature, h is the Planck constant and k_B is the Boltzmann constant.

For the protein binding with and without ligand binding, the rigidified dihedral angles are different and cause various atom position Jacobian matrix. So the protein binding with and without ligands has different vibrational frequencies and entropy. The change of vibrational entropy is derived as

$$\Delta S_{vib} = S_{vib,pl} - S_{vib,p} \quad (5)$$

¹Atomwise, Inc. 717 Market Street, San Francisco, CA 94103 USA

²Department of Bioengineering and Therapeutic Sciences, UCSF, California, USA

We compute the vibrational entropy for 34 pdbfiles and compare the results with the experimental data from the NMR [4] to validate the results. As shown in the Fig. 1, our method can accurately predict the vibrational entropy change for the protein-ligand binding. The Pearson correlation factor r_P is used to show the correlation between the experimental data and numerical results. The correlation factor of our numerical results is 0.80, thus our numerical results do well fit the experimental data.

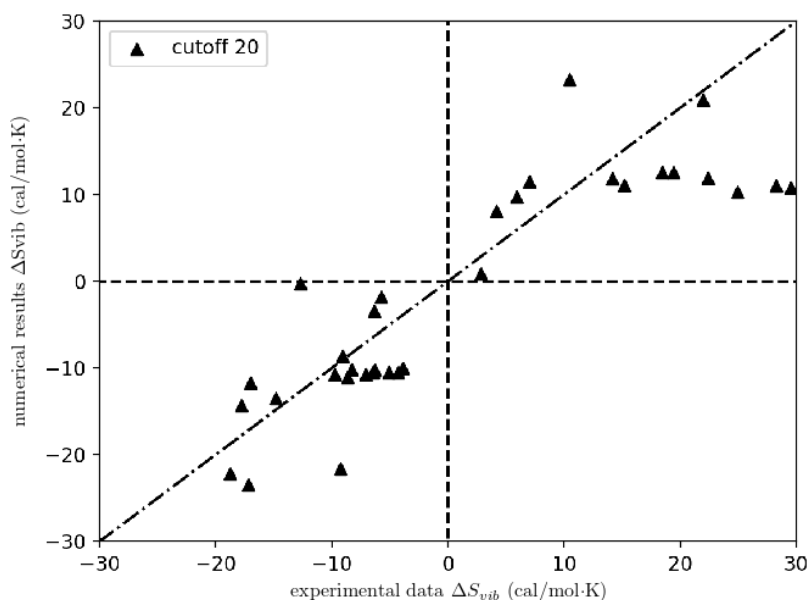


Figure 1: Comparison of experimental data from [4] and numerical results (distance cutoff from 20Å) for change of vibrational entropy binding with and without ligands. The Pearson correlation factor is used to present the relation between numerical and experimental data. The Pearson correlation factor is $r_P = 0.80$

References

- [1] Budday, Dominik and Leyendecker, Sigrid and van den Bedem, Henry. Geometric analysis characterizes molecular rigidity in generic and non-generic protein configurations. *Journal of the Mechanics and Physics of Solids*, Vol. 83, p. 36-47, 2015.
- [2] Budday, Dominik and Leyendecker, Sigrid and van den Bedem, Henry. Kinematic Flexibility Analysis: Hydrogen Bonding Patterns Impart a Spatial Hierarchy of Protein Motion. *Journal of Chemical Information and Modeling*, Vol. 58, p. 2108-2122, 2018.
- [3] Mendez, Raul and Bastolla, Ugo. Torsional Network Model: Normal Modes in Torsion Angle Space Better Correlate with Conformation Changes in Proteins. *Physical Review Letters*, Vol. 104, 2010.
- [4] Gohlke, Holger and Ben-Shalom, Ido Y. and Kopitz, Hannes and Pfeiffer-Marek, Stefania and Baringhaus, Karl-Heinz. Rigidity Theory-Based Approximation of Vibrational Entropy Changes upon Binding to Biomolecules. *Journal of Chemical Theory and Computation*, Vol. 13, p. 1495-1502, 2017.

Modelling the characteristic orthotropic tissue structure in the myocardium

David Holz, Minh Tuan Duong, Denisa Martonová, Muhannad Alkassar¹, Sigrid Leyendecker

Various approaches for assigning the orthotropic tissue structure to a finite element model have been proposed. While some approaches directly base on postprocessed imaging data e.g. using DT-MRI or histology, most of the nowadays used cardiac models utilise a rule-based method in order to give the finite element domain the characteristic orthotropic property of the myocardium. However, often rule-based approaches rely on the correct assessment of the transmural depth from the endocardium to the epicardium. Many of the existing strategies are not able to give an appropriate assessment of the transmural depth. We propose a method based on a discontinuous Galerkin approach in order to assess the ventricular myocardial thickness (transmural depth e) [1, 3, 2]. In Figure 1, we show the visualisation of the fibre orientation from a cutout of the left ventricle with a fibre angle varying linearly from -60 (blue ●) to +60 (red ●) degree. In Figure 2, the local fibre orientation in a hollow cylinder is shown, which varies from -60 (blue ●) to +60 (red ●) degree.

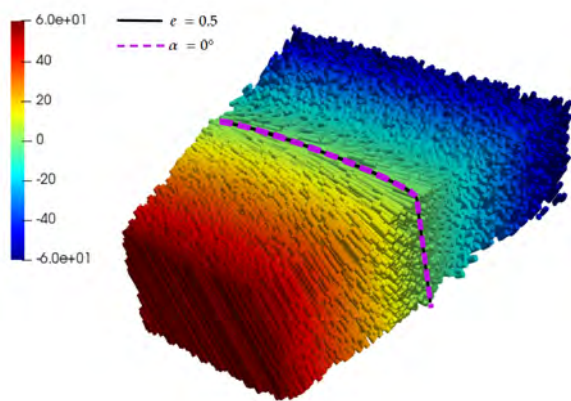


Figure 1: cutout – LV

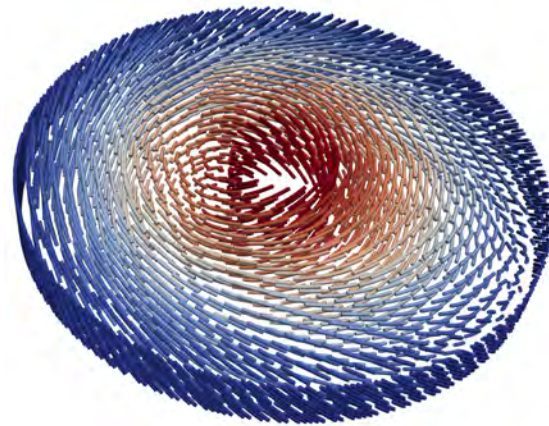


Figure 2: fibre orientation – hollow cylinder

In Figure 1, the fibre orientation of a cutout from the left ventricle is shown. The fibre angle is varying linearly from -60 (blue ●) to +60 (red ●) degree. In Figure 2, a streamline visualisation of a hollow cylinder is shown, which varies linearly from -60 (blue ●) to +60 (red ●).

Acknowledgment This work is funded by the Klaus Tschira Stiftung grant 00.289.2016

References

- [1] S. E. Jones, B. R. Buchbinder, I. Aharon. *Three-dimensional mapping of cortical thickness using Laplace's equation*. Human brain mapping **11:1**, 12–32 (2000).
- [2] J. D. Bayer, R. C. Blake, G. Plank, N. A. Trayanova. *A novel rule-based algorithm for assigning myocardial fiber orientation to computational heart models* Annals of biomedical engineering **40:10**, 2243–2254 (2012).
- [3] F. Brezzi, L. D. Marini, E. Süli. *Discontinuous Galerkin methods for first-order hyperbolic problems* Mathematical models and methods in applied sciences **14:12**, 1893–1903 (2004).

¹Pediatric Cardiology, Friedrich-Alexander-Universität Erlangen-Nürnberg, Loschgestrasse 15, 91054 Erlangen, Germany

Electromechanically coupled beam models for stacked dielectric elastomer actuators

Dengpeng Huang, Sigrid Leyendecker

In this project, we are interested in developing the actuators for soft robotics. It has many advantages over traditional robots such as the flexible bionic structure, powerful task-capability and safe interaction with environment. To this end, the Dielectric Elastomer Actuators (DEAs) have been developed to perform as the artificial muscles for the soft robotics, see e.g. [1]. The DEA possesses the sandwiched structure, where the dielectric elastomer is sandwiched between two compliant electrodes, as shown in Fig.1. When the external electrical field is applied, the contraction of the DEA will be induced by the polarizing of the dielectric elastomer. When the larger deformation is required, the stacked DEA with multiple capacitors can be applied.

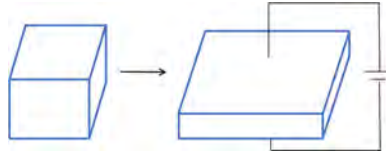


Figure 1: Working principle of DEA.

The deformation behavior of the DEA is governed by the electromechanical coupling in the balance law of momentum and the Maxwell equations, see e.g. [2, 3]. The governing equations in continuum mechanics and the geometrically exact beam can formulated as seen below.

<p>Maxwell equation</p> $\begin{aligned} \nabla_{\mathbf{X}} \times \mathbf{E}^e &= \mathbf{0}, & \nabla_{\mathbf{X}} \cdot \mathbf{D} &= 0 & \text{in } B \\ \mathbf{D} \cdot \mathbf{n} &= \hat{q} & \text{on } \partial B_q \\ \phi &= \hat{\phi} & \text{on } \partial B_\phi \end{aligned}$	<p>Maxwell equation in beam</p> $\begin{aligned} \partial_s d_s^e + d^{e,ext} &= 0 & \text{in } B \\ \mathbf{d}^e \cdot \mathbf{n} &= \hat{q} & \text{on } \partial B_q \\ \phi &= \hat{\phi} & \text{on } \partial B_\phi \end{aligned}$
<p>Balance of momentum</p> $\begin{aligned} \nabla_{\mathbf{X}} \cdot \mathbf{P} + \rho_0 \bar{\mathbf{b}} &= \rho_0 \ddot{\mathbf{u}} & \text{in } B \\ \mathbf{F} \mathbf{P}^T &= \mathbf{P} \mathbf{F}^T & \text{in } B \\ \mathbf{P} \mathbf{N} &= \hat{\mathbf{t}} & \text{on } \partial B_\sigma \\ \mathbf{u} &= \hat{\mathbf{u}} & \text{on } \partial B_u \end{aligned}$	<p>Balance of momentum in beam</p> $\begin{aligned} \partial_s \mathbf{f} + \mathbf{f}^{ext} &= \rho A \ddot{\mathbf{u}} & \text{in } B \\ \mathbf{f}^{ext} &= \hat{\mathbf{t}} & \text{on } \partial B_\sigma \\ \mathbf{u} &= \hat{\mathbf{u}} & \text{on } \partial B_u \\ \partial_s \mathbf{m} + \partial_s \mathbf{u} \times \mathbf{f} + \mathbf{m}^{ext} &= \mathbb{I} \dot{\boldsymbol{\omega}} + \boldsymbol{\omega} \times \mathbb{I} \boldsymbol{\omega} \end{aligned}$
$\Omega_b(\boldsymbol{\gamma}, \boldsymbol{\kappa}, \boldsymbol{\varepsilon}) = \int_{\Sigma} \Omega(\mathbf{C}, \mathbf{E}^e) dA$	

with \mathbf{E}^e the electrical field, \mathbf{D} the electric displacement in the initial configuration, ϕ the current electric potential, \mathbf{P} the first Piola-Kirchhoff stress tensor, ρ_0 the mass density in initial configuration, $\bar{\mathbf{b}}$ the body force vector, $\ddot{\mathbf{u}}$ the acceleration, \mathbf{F} the deformation gradient, Ω the strain energy, $\mathbf{d}^e = [d_1^e \ d_2^e \ d_s^e]^T$ the electric displacement vector for beam, \mathbf{f} the internal force, \mathbf{f}^{ext} the external force, $\boldsymbol{\omega}$ the spatial angular velocity, \mathbb{I} the spatial mass moment of inertia tensor, \mathbf{m} the torque per unit of arch-length, Ω_b the strain energy per unit arc-length in beam, $\boldsymbol{\varepsilon}$ the strain-like electric variable conjugated with the electric displacement \mathbf{d}^e of beam, $\boldsymbol{\gamma}$ and $\boldsymbol{\kappa}$ the beam strain measures.

By applying proper electric potential as boundary conditions on the beam cross sections, different modes of deformation in the beam are generated, such as contraction, shear, bending and torsion as shown in Fig.2. The beam model is validated by comparing the results with the 3D finite element model.

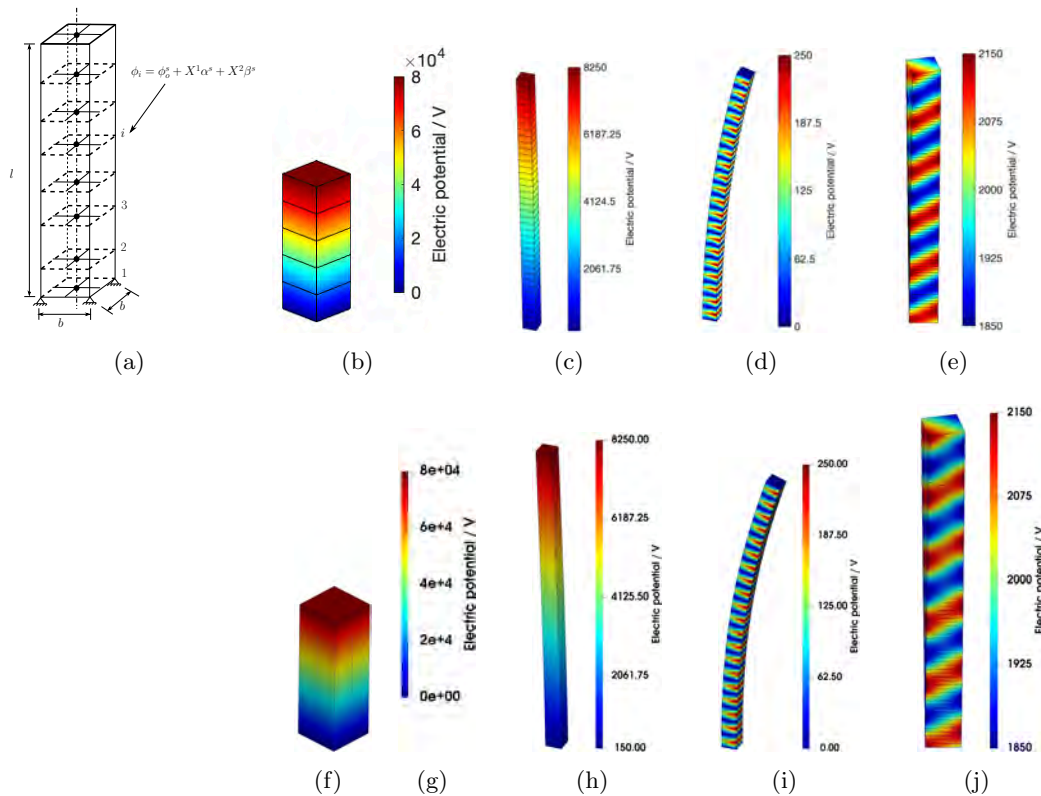


Figure 2: Simulation of DEA with (a) initial geometry, (b) contraction, (c) shear, (d) bending, (e) torsion by beam model, and (f)-(j) by 3D FEM model.

References

- [1] M. Duduta, E. Hajiesmaili, H. Zhao, R. J. Wood, and D. R. Clarke. Realizing the potential of dielectric elastomer artificial muscles. *Proceedings of the National Academy of Sciences*, 116(7):2476-2481, 2019.
- [2] D. Vu, P. Steinmann, and G. Possart. Numerical modelling of non-linear electroelasticity. *International Journal for Numerical Methods in Engineering*, 70(6):685-704, 2007.
- [3] T. Schloegl and S. Leyendecker. Electrostatic viscoelastic finite element model of dielectric actuators. *Computer Methods in Applied Mechanics and Engineering*, 299:421-439, 2016.

Investigation of optical motion capturing for characterizing movement patterns of the hand in rheumatoid arthritis

Michael Klebl, Uday Phutane, Anna-Maria Liphardt, Johann Penner and Sigrid Leyendecker

Introduction The diagnosis of Rheumatoid arthritis (RA), a chronic inflammatory auto-immune disease, and assessment is mainly done using patient reported outcome measures, such as questionnaires and simple validated functional tests like isometric grip strength or the Moberg-Picking-Up Test (MPUT, [2]) which can be used to quantify muscle performance and fine motor skills but do not allow identifying and quantifying differences in movement patterns. These functional measures, even though they are objective, often are greatly affected by age and sex in RA patients. A detailed quantification of hand function capturing simple tasks but also complex movements that can reflect subjectively observed hand function impairment in patients with RA would be desirable, which was done by an optoelectronic measurement systems (OMS) [3].

methods Individuals diagnosed with RA and healthy controls were included in the study, see [3]. The assessment of clinical hand function included several tests. First of all, isometric grip strength was measured in pounds (lbs) using a hand dynamometer (Lafayette Instrument, Lafayette, IN, USA). Three measurements of grip strength were performed, starting with the dominant hand and alternating between hands. The highest measured force for each hand was included in the data analysis. Secondly, fine motor skills were assessed using the Moberg-Picking-Up test [2]. Briefly, subjects are asked to pick up twelve small items and drop them into a box as fast as possible while the time to complete the task is recorded. With each hand two repetitions of the test were completed starting with the dominant hand. The fastest trial was included in the analysis. Hand segment kinematics were recorded with synchronized and calibrated high-resolution and high-speed infrared cameras (eight Oqus7+ cameras and one Oqus5+ camera, Qualisys AB, Sweden) by tracking 29 retroreflective spherical markers with diameters of 8 mm and 14 mm at a frame-rate of 100 Hz, as seen with different hand postures in Figure 1. The markers were placed on the hand dorsum using double-sided hypoallergenic adhesive tape, based on anatomical landmarks according to the layout described in [1].

results Forty-seven individuals participated in this study [3]. This provided us with measurement data for $N_A = 64$ total hands with $N_C = 35$ healthy controls and $N_R = 29$ RA patients hands. MPUT and grip strength results for clinical and OMS setup are summarized in Table 1. The mean MPUT time in the clinical setting was significantly slower in RA patients (17.5 ± 4.7 s) compared to control subjects (14.1 ± 4.1 s). Mean MPUT times with markers during OMS data collection was 20.3 ± 7.1 s for RA patients and 16.0 ± 4.5 s for the control group. This increase in MPUT times is similar for control and RA participants and also for men and women. The mean, standard deviation, maximum and minimum values values for MPUT and grip strength test are provided in Table 1.

Table 1: The table provides the mean (sd, or standard deviation), minimum, and maximum values for subjects' grip strength and times for MPUT in the clinical setting and with the OMS setup.

		ALL ($N_A = 64$)			CON ($N_C = 35$)			RA ($N_R = 29$)		
		min	mean (sd)	max	min	mean (sd)	max	min	mean (sd)	max
grip strength in lbs	clinical	32	82.3 (34.6)	178	44	91.7 (35.7)	178	32	71.8 (29.8)	134
	OMS	19	64.0 (28.6)	140	19	71.5 (29.6)	140	20	55.4 (24.7)	102
MPUT times in s	clinical	9.2	15.6 (4.7)	31.4	9.2	14.1 (4.1)	31.4	12.2	17.5 (4.7)	30.1
	OMS	11.1	18.0 (6.2)	41.0	11.1	16.0 (4.5)	31.9	12.2	20.3 (7.1)	41.0

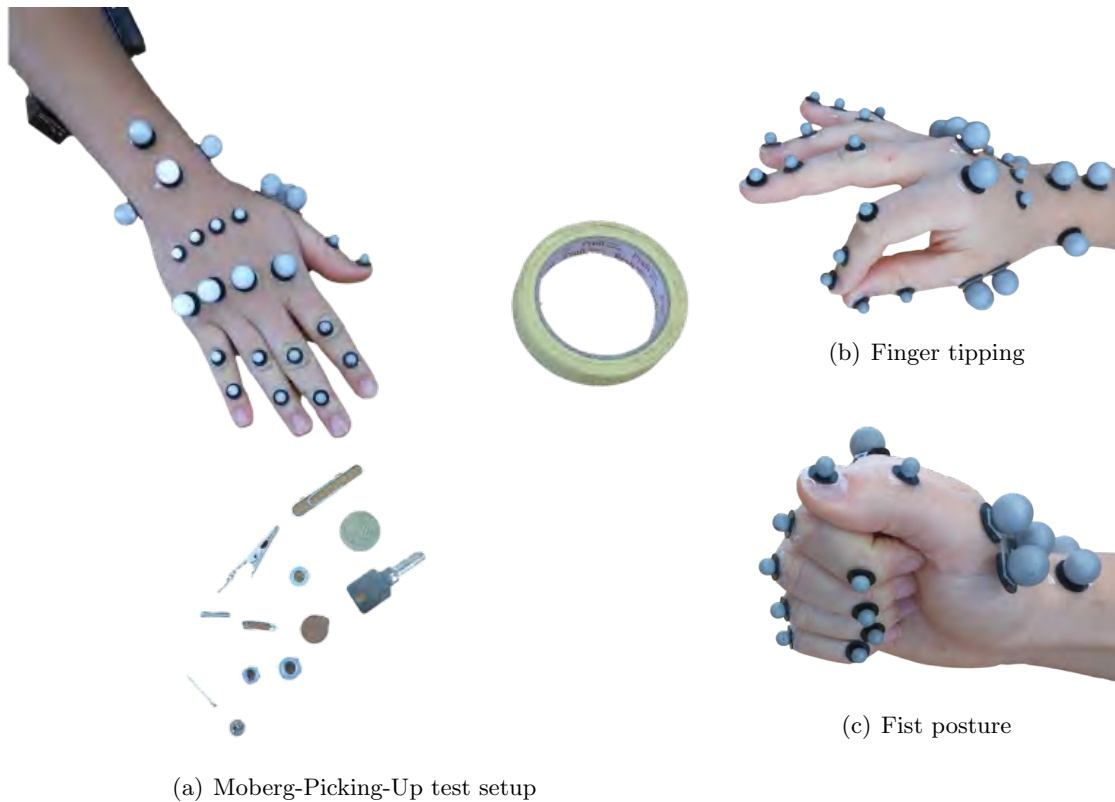


Figure 1: The hand postures for the different recordings, with the respective marker set-up. The participants are instructed to lift and place 12 objects in the nearby container. In (b), finger tipping motion is shown between the thumb and the index finger. In (c), the fist posture showing the full flexion capacity of the hand is demonstrated.

conclusion The investigation emphasizes the need for adapting newer technologies to assist in the characterization of hand movement in patients suffering from RA. To achieve this, the integration of existing clinical methodologies together with state of the art technologies and experimental methodology is essential. Optical tracking using OMS has been shown capable of capturing a variety of hand movements observed in activities of daily living. Furthermore, hand movement maybe artificially changed because of restrictions due to markers mounted on the skin and the artificial test environment. To acquire hand function in a more natural environment, markerless capturing of movement is desirable.

References

- [1] J.L. Sancho-Bru, N.J. Jarque-Bou, M. Vergara, A. Perez-Gonzalez, *Validity of a simple videogrammetric method to measure the movement of all hand segments for clinical purposes*. Proc. Inst. Mech.Eng Part H: J Engineering in Medicine 228(2), 2014, 182-9.
- [2] NC.L. Ng, D.D. Ho, S.P. Chow, *The Moberg pickup test: results of testing with a standard protocol*. Journal of Hand Therapy 12(4), 1999, 309-12.
- [3] U.Phutane, A.M. Liphardt, J. Bräunig, J. Penner, M. Klebl, M. Vossiek, A. Kleyer, G. Schettband, S. Leyendecker. *Investigation of Optical and Radar Based Motion Capturing Technologies for Characterizing Movement Patterns of the Hand in Rheumatoid Arthritis*. Biosensors, 2020 (in review).

Discrete mechanics for static Cosserat rods with forcing

Holger Lang, Sigrid Leyendecker, Joachim Linn

The kinematics of a **continuous Cosserat rod** [2] is completely determined by its centerline $\mathbf{x} : [0, L] \rightarrow \mathbb{R}^3$ and a centerline fixed frame $\mathbf{R} = [d^1, d^2, d^3] : [0, L] \rightarrow SO(3)$, which is specifying the cross section orientation. See Figure 2. With the strain $\mathbf{\Gamma} = \mathbf{R}^\top \partial_s \mathbf{x} - \mathbf{e}_3$ and the curvature $\mathbf{K} = \mathbf{R}^\top \partial_s \mathbf{R}$, the elasticity matrices $\mathbf{C}_\Gamma = \text{diag}(GA, GA, EA)$ and $\mathbf{C}_K = \text{diag}(EI_1, EI_2, GJ)$, and the coordinates $\mathbf{q} = (\mathbf{x}, \mathbf{R})$, the internal elastic energy can be expressed as

$$\mathcal{V} = \int_0^L \mathcal{W}(\mathbf{q}, \mathbf{q}') ds, \quad \mathcal{W}(\mathbf{q}, \mathbf{q}') = \frac{1}{2} \mathbf{\Gamma}^\top \mathbf{C}_\Gamma \mathbf{\Gamma} + \frac{1}{2} \mathbf{K}^\top \mathbf{C}_K \mathbf{K}.$$

In analogy of Lagrangian dynamic systems, \mathcal{V} can be interpreted as the action, \mathcal{W} as the Lagrangian function of the system. Forces and moments are related via $\mathbf{f} = \mathbf{R} \mathbf{C}_\Gamma \mathbf{\Gamma}$ resp. $\mathbf{m} = \mathbf{R} \mathbf{C}_K \mathbf{K}$ to the strain resp. curvature.

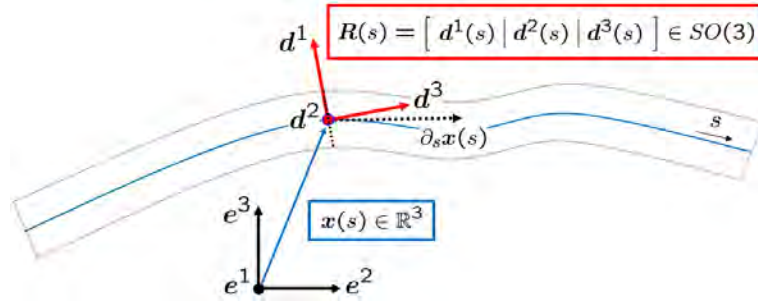


Figure 2: Kinematics of a Cosserat rod

The stationarity of the action functional leads to the continuous static equilibrium equations

$$\begin{cases} \mathbf{0} &= \mathbf{T}(\mathbf{q})^\top \left\{ \frac{d}{ds} \nabla_{\mathbf{q}'} W(\mathbf{q}, \mathbf{q}') - \nabla_{\mathbf{q}} W(\mathbf{q}, \mathbf{q}') \right\}, \\ \mathbf{0} &= \mathbf{g}(\mathbf{q}) \end{cases},$$

where $\mathbf{T}(\mathbf{q})$ is a null space matrix to the constraint function $\mathbf{g}(\mathbf{R}) = \mathbf{R}^\top \mathbf{R} - \mathbf{E}$, see e.g. [2].

Noether's Theorem [1] yields the following conserved magnitudes: The total force $\mathbf{f}(s)$ (since \mathcal{W} is translatory invariant), the total momentum $\mathbf{m}(s) + \mathbf{x}(s) \times \mathbf{f}(s)$ (since \mathcal{W} is rotatory invariant) and the twist moment $\langle \mathbf{m}(s), \mathbf{d}^3(s) \rangle$ (in case that \mathcal{W} is isotropic, i.e., if $EI_1 = EI_2$). Here, $s \in [0, 1]$.

Similarly as in [2], a consistent **discrete Cosserat rod** can be defined by the discrete centroids $\mathbf{x}_n \in \mathbb{R}^3$ and discrete cross section orientations $\mathbf{R}_n \in SO(3)$, both situated on a discrete node (or vertex) grid $0 = s_0 < s_1 < \dots < s_N = L$. With the discrete strains $\mathbf{\Gamma}_\nu = \frac{1}{2\Delta s_\nu} (\mathbf{R}_{\nu-\frac{1}{2}} + \mathbf{R}_{\nu+\frac{1}{2}})^\top (\mathbf{x}_{\nu+\frac{1}{2}} - \mathbf{x}_{\nu-\frac{1}{2}}) - \mathbf{e}_3$ and the discrete curvatures $\hat{\mathbf{K}}_\nu = \frac{1}{\Delta s_\nu} \text{inv cay}(\mathbf{R}_{\nu-\frac{1}{2}}^\top \mathbf{R}_{\nu+\frac{1}{2}})$, where $\Delta s_\nu = s_{\nu+1/2} - s_{\nu-1/2}$ and $\nu = \frac{1}{2}, \dots, N - \frac{1}{2}$, the discrete internal elastic energy can be written as

$$V = \sum_{\nu=1/2}^{N-1/2} W_\nu \Delta s_\nu, \quad W_\nu = \frac{1}{2} \mathbf{\Gamma}_\nu^\top \mathbf{C}_\Gamma \mathbf{\Gamma}_\nu + \frac{1}{2} \mathbf{K}_\nu^\top \mathbf{C}_K \mathbf{K}_\nu.$$

The stationarity of this discrete action leads to the discrete static equilibrium equations

$$\begin{cases} \mathbf{0} &= \mathbf{T}(\mathbf{q}_n)^\top \{ \nabla_l W(\mathbf{q}_n, \mathbf{q}_{n+1}) + \nabla_r W(\mathbf{q}_{n-1}, \mathbf{q}_n) \}, \\ \mathbf{0} &= \mathbf{g}(\mathbf{q}_n) \end{cases},$$

where ∇_l resp. ∇_r denote the gradient w.r.t. the left resp. right argument. Internal forces and momenta are obtained via the discrete Legendre transformation

$$\begin{bmatrix} \mathbf{f}_n \\ \mathbf{m}_n \end{bmatrix} = - \begin{bmatrix} \mathbf{E} & \\ & \mathbf{T}(\mathbf{q}_n)^\top \end{bmatrix} \nabla_l W(\mathbf{q}_n, \mathbf{q}_{n+1}) = \begin{bmatrix} \mathbf{E} & \\ & \mathbf{T}(\mathbf{q}_n)^\top \end{bmatrix} \nabla_r W(\mathbf{q}_{n-1}, \mathbf{q}_n).$$

The discrete Noether Theorem [1] now yields the following conserved magnitudes: The total force \mathbf{f}_n (since W is translatory invariant), the total momentum $\mathbf{m}_n + \mathbf{x}_n \times \mathbf{f}_n$ (since W is rotatory invariant) and the twist moment $\langle \mathbf{m}_n, \mathbf{d}_n^3 \rangle$ (in case that W is isotropic). Here $n = 0, 1, 2, \dots, N$. According to the discrete Lagrange-d'Alembert principle, exterior forces \mathbf{F}_L and moments \mathcal{M}_L at $s = L$ can be added to the right-hand side of the equilibrium equations, yielding

$$\begin{cases} \mathbf{0} &= \mathbf{T}^\top(\mathbf{q}_n) \{ \nabla_l W(\mathbf{q}_n, \mathbf{q}_{n+1}) + \nabla_r W(\mathbf{q}_{n-1}, \mathbf{q}_n) \} \\ \mathbf{0} &= \mathbf{T}^\top(\mathbf{q}_N) \{ \nabla_r W(\mathbf{q}_{N-1}, \mathbf{q}_N) \} + \begin{bmatrix} \mathcal{F}_L \\ \mathcal{M}_L \end{bmatrix} \\ \mathbf{0} &= \mathbf{g}(\mathbf{q}_n) \end{cases}$$

for $n = 1, \dots, N$. See Figure 1 for the conserved quantities for a scenario, where the boundary conditions $\mathbf{x}_0 = \mathbf{0}$, $\mathbf{R}_0 = \mathbf{E}$, $\mathcal{F}_L = [1.0, 2.0, 3.0]^\top$, $\mathcal{M}_L = [4.0, 5.0, 6.0]^\top$ are imposed and the parameters $L = 1$, $EI_1 = EI_2 = GJ = 1$, $GA = EA = 200$ are used. $N = 40$ elements are chosen.

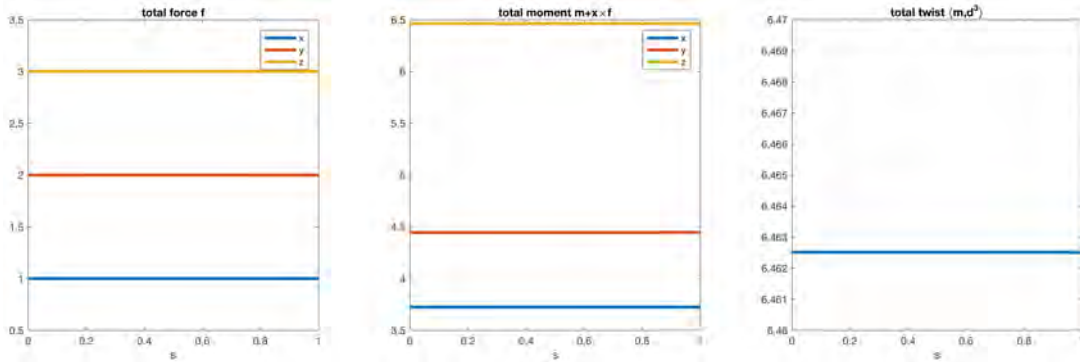


Figure 3: Above: Perfect conservation of the total force, the total moment and the twist moment. The defects are of maximum order 10^{-12} .

Whereas the left-boundary forces \mathbf{f}_0 do not depend on the solution ($\mathbf{f}_0 = \mathbf{f}_1 = \dots = \mathbf{f}_N = \mathcal{F}_L$), the left-boundary moments \mathbf{m}_0 depend on the (non trivial) deformed configuration and therefore on the grid size Δs_ν . (In discrete Lagrangian dynamics, we typically have an initial value problem, from which the values of the conserved quantities are determined from the initial values. They are independent of the time grid resolution.) In beam statics, the conserved quantities are configuration dependent, their values depending on the spatial grid. However, convergence to the continuum limit is obtained for grid refinement.

References

- [1] J.E. Marsden, M. West, “Discrete mechanics and variational integrators”, *Acta Numerica*, Vol. 10, pp. 357-514, 2001.
- [2] P. Jung, S. Leyendecker, J. Linn, M. Ortiz, “A discrete mechanics approach to the Cosserat rod theory - Part 1: static equilibria”, *Int. J. Numer. Meth. Engng.*, Vol. 85, pp. 31-60, 2009.

First steps towards a cardiac assist device to support a diseased rat heart

D. Martonová, D. Brackenhauer, D. Holz, M. Landgraf¹, M. Alkassar¹, S. Leyendecker

If a heart is seriously diseased, there are usually only two options – the use of a cardiac assist device (CaAD) or heart transplantation. In the last decades, many CaADs have been developed, including those with and without a direct blood contact. So far, the latter can only support a heart during the active contraction (systole) by generating a positive support pressure on the epicardium [3]. In this work, we consider first steps towards the modelling and simulation of a CaAD without the blood contact supporting a heart during the systole via a positive support pressure facilitating the ventricular outflow as well as during the diastole via a negative support pressure which relieves the diastolic filling.

Simple modelling approach

On the epicardium of a generic finite element model of the rat left ventricle (LV), see Figure 1 left, a sinusoidal support pressure $p(t)$ as displayed in Figure 1 middle is applied. In order to model a diseased heart, e.g. after myocardial infarction, the ventricular stiffness in the strain energy function for the passive myocardium [2] is increased and the maximal active force in the model [1] is decreased. The resulting pressure-volume loops are presented in Figure 1 right. By applying a negative pressure during the diastole and a positive pressure during the systole, we observe a significant increase in the ejection fraction, namely from 41% in the diseased case to 58% which lies in the physiological range.

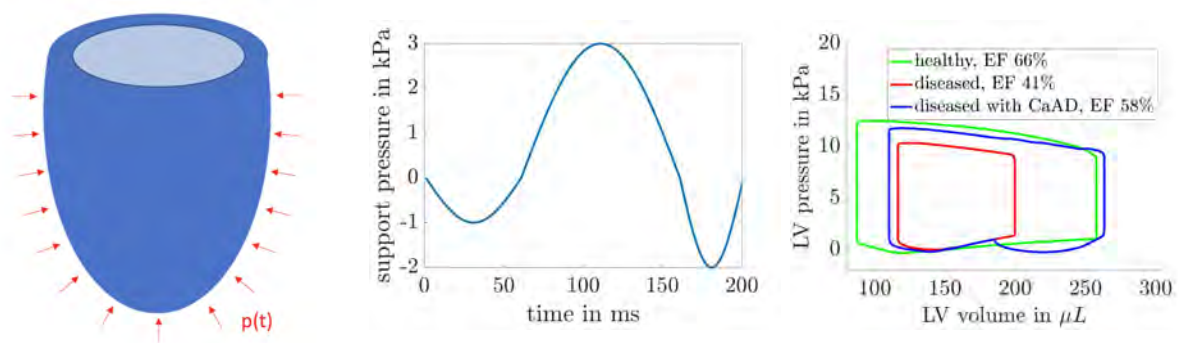


Figure 1: Left: generic LV with support pressure $p(t)$. Middle: temporal evolution of support pressure $p(t)$. Right: simulated pressure-volume loops for healthy rat LV and diseased rat LV with and without CaAD generating a support pressure $p(t)$.

Acknowledgments This work is funded by the Klaus Tschira Stiftung grant 00.289.2016.

References

- [1] J. M. Guccione, L. K. Waldman, A. D. McCulloch. *Mechanics of Active Contraction in Cardiac Muscle: Part II—Cylindrical Models of the Systolic Left Ventricle*. J. Biomech. Eng. **82(90)**, 115 (1993).
- [2] G.A. Holzapfel, and R.W. Ogden. *Constitutive modelling of passive myocardium: a structurally based framework for material characterization*. Phil. Trans. R. Soc. A. **367**, 3445–3475 (2009).
- [3] A. A. Bakir, A. A. Abed, M. C. Stevens, N. H. Lovell, S. Dokos. *A Multiphysics Biventricular Cardiac Model: Simulations With a Left-Ventricular Assist Device*. Front. Physiol. **9** (2018).

¹Pediatric Cardiology, Friedrich-Alexander-Universität Erlangen-Nürnberg, 91054 Erlangen, Germany

Musculoskeletal optimal control simulations with a discrete muscle wrapping formulation and improved contact modelling

Johann Penner, Sigrid Leyendecker

In this work, we investigate a simulation model for the human musculoskeletal system, which shall be steered from a certain initial state to a predefined final state in an optimal way. These optimal control simulations require the prediction of the action of muscles working around joints, in conjunction with skeletal movements that are represented as a multibody system. In particular, we are interested in a formulation for the direct contact between muscles and any number of wrapping surfaces that enables contact opening. Therefore, we employ the direct transcription method DMOCC [2] along with a discrete muscle path formulation and the Signorini contact problem. This enables us to solve the transcribed constrained minimisation problem to find control trajectories simultaneously with an inequality complementarity contact behaviour. The result is an improved musculoskeletal optimal control simulation model with a contact formulation that requires less foreknowledge of the wrapping surfaces than in previous work, see [3, 4].

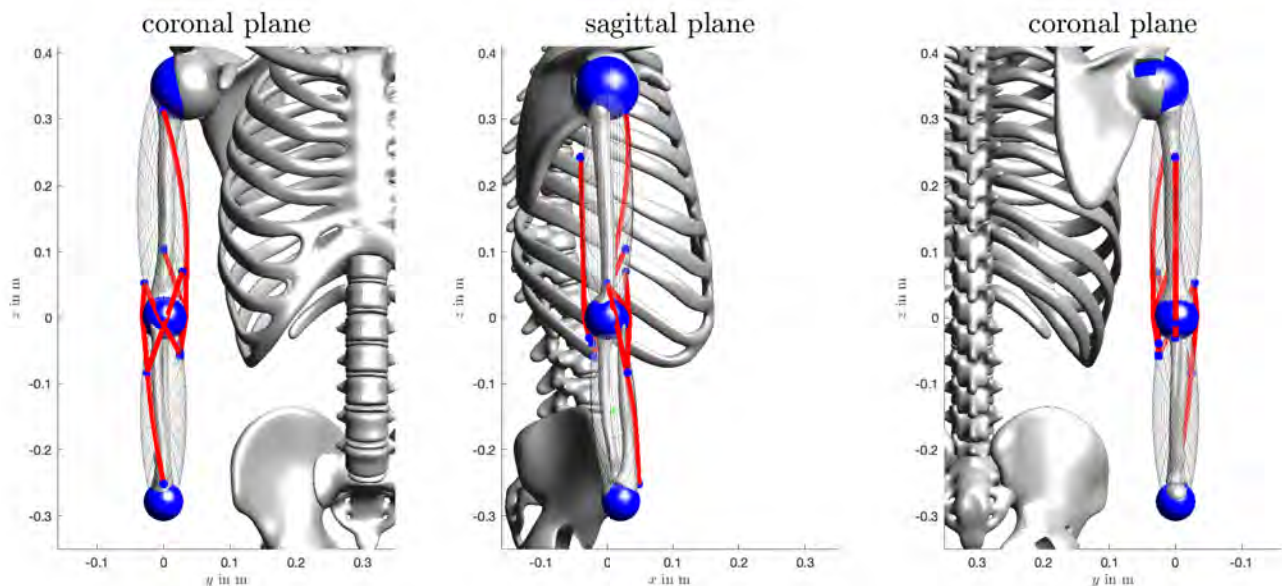


Figure 1: Musculoskeletal arm model with major muscles around the elbow¹

All formulations in this work are based on discrete Lagrangian mechanics, including skeletal dynamics and muscle paths. This requires the discretization of all continuous quantities in Hamilton's principle. The resulting discrete Euler-Lagrange equations are time stepping equations that inherit certain characteristic properties of the continuous solution. Finally, the structure preserving properties of the integrator enable our simulations to account for large, rapid changes in muscle paths, and skeleton dynamics [3, 2].

The DMOCC [2] method then deals with the problem of finding discrete optimal control trajectories subject to the discrete Euler-Lagrange equations of the system, such that a certain discrete objective function J_d , or respectively the sum of a discrete cost function C_d , with respect to a discrete optimisation vector $\mathbf{x}_d = \{\mathbf{x}_n\}_{n=0}^N$ with $N \in \mathbb{N}$ and $N + 1$ time nodes is minimised. The optimal control

¹3d bone geometry from <https://www.thingiverse.com/thing:1543880>

problem in this work reads

$$\min_{\mathbf{x}_d} J_d(\mathbf{x}_d) = \min_{\mathbf{x}_d} \sum_{n=0}^{N-1} C_d(\mathbf{x}_n, \mathbf{x}_{n+1})$$

· discrete Lagrange mechanics
 subject to · geodesic muscle paths
 · Signorini problem
 · boundary and path conditions

where the infinite dimensional optimal control problem is transcribed into a finite dimensional non-linear programming problem that can be solved by any suitable standard algorithm.

The point of using discrete Lagrangian mechanics is that we intend to use a structure preserving integration method. In general, arbitrary time discretization methods do not inherit the conserved quantities in the solution of the equations of motion. However, the discretization of the Hamilton principle is able to inherit symmetries of the continuous dynamical system and consequently inherits its structure preserving properties. In addition, the resulting variational integrator shows very good energy behaviour with a limited energy error in long time simulations, which is very advantageous for our simulations [3, 2].

To define the shortest path problem over a given obstacle, we first assume that the muscle completely touches the surfaces, thus the path is constrained by a holonomic surface constraint $\phi(\gamma_k) = 0 \in \mathbb{R}$. We define the discrete geodesic curve $\gamma_d = \{\gamma_k\}_{k=0}^K$ on a discrete arc length grid with $K \in \mathbb{N}$ and $K+1$ nodes. Here, a discrete geodesic curve has to satisfy the geodesic discrete Euler-Lagrange equations

$$\frac{\partial L_\gamma(\gamma_{k-1}, \gamma_k)}{\partial \gamma_k} + \frac{\partial L_\gamma(\gamma_k, \gamma_{k+1})}{\partial \gamma_k} - \Phi_d(\gamma_k)^T \cdot \lambda_k = \mathbf{0} \quad \text{for} \quad k = 1, \dots, K-1$$

where $\Phi_d(\gamma_k)$ is the discrete surface Jacobian and $\lambda_k \in \mathbb{R}$ is a Lagrange multiplier, see [3, 4].

Now, the frictionless contact between muscle path and surface is described via the Signorini problem. The relation between the relative distance $\phi(\gamma_k)$ and the Lagrange multiplier λ_k constitutes an inequality complementarity behaviour

$$\phi(\gamma_k) \geq 0 \quad \lambda_k \geq 0 \quad \phi(\gamma_k)^T \cdot \lambda_k = 0$$

which defines the contact between muscle path and adjacent wrapping surface and can handle possible contact opening and closing. This concludes the non-linear programming problem for our musculoskeletal optimal control simulations.

References

- [1] Leyendecker, S.; Marsden, J.E.; Ortiz, M.: Variational integrators for constrained dynamical systems. ZAMM-Journal of Applied Mathematics and Mechanics, Vol. 88, p. 677-708, 2008.
- [2] Leyendecker, S.; Ober-Bloebaum, S.; Marsden, J.E.; and Ortiz M.: Discrete mechanics and optimal control for constrained systems. Optimal Control Applications and Methods, Vol. 31, p. 505-528, 2010.
- [3] Penner, J.; Leyendecker, S.: Multi-Obstacle Muscle Wrapping Based on a Discrete Variational Principle. In I. Farago, F. Izsok, P.L. Simon (Ed.) Progress in Industrial Mathematics at ECMI 2018, p. 223-229, Springer, 2019.
- [4] Penner, J.; Leyendecker, S.: A Hill Muscle Actuated Arm Model with Dynamic Muscle Paths. In A. Kecskemethy, F. Geu Flores (Ed.) Multibody Dynamics 2019. Computational Methods in Applied Sciences, pp. 52-59, Springer, 2020.

Spatially varying regularisation variable in quasi-static phase-field model for brittle fractures

Dhananjay Phansalkar, Michael Ortiz¹, Kerstin Weinberg², Sigrid Leyendecker

Broadly, there are two computational modeling methodologies in fracture mechanics, namely discrete and diffusive crack approaches. In many cases, the discrete crack approaches are algorithmically complex, computationally expensive or both. In contrast, the diffusive crack approach, is quite simple to implement in the existing finite element libraries. Over the last decade, this method has been extensively developed for various material models and complex applications. However, there are a few issues associated with this method. It is known to suffer from convergence issues with the Newton method for monolithic approaches [1]. This approach is reliant on a regularisation parameter ϵ , under the requirement that $h \ll \epsilon$, where h is the mesh size parameter. Therefore, at lower ϵ the necessity of finer meshes can make it computationally expensive. Moreover, the actual solution of the numerical problem can be dependent on h itself. Our work strives to develop a formulation with spatially varying ϵ to alleviate mesh dependency, lowering the cost of this approach and making it more accessible. The total energy in the system given by the standard phase field model is

$$E(\mathbf{u}, c) = \int_{\Omega} [1 - c]^2 \psi(\boldsymbol{\epsilon}) + \mathcal{G}_c \left[\frac{c^2 + \eta}{2\epsilon} + \frac{\epsilon}{2} |\nabla c|^2 \right] \mathbf{d}x \quad (1)$$

$$\psi(\boldsymbol{\epsilon}) = \frac{1}{2} \boldsymbol{\epsilon}(\mathbf{u}) : [\mathbb{C} \boldsymbol{\epsilon}(\mathbf{u})] = \frac{1}{2} \lambda [\text{tr}(\boldsymbol{\epsilon})]^2 + \mu [\boldsymbol{\epsilon} : \boldsymbol{\epsilon}]$$

where \mathbf{u} , c , and $\boldsymbol{\epsilon}$ are the displacement, phase field and strain respectively, ϵ is a constant regularisation parameter, and \mathcal{G}_c , λ and μ are material parameters. It has been shown that in the limit $\epsilon \rightarrow 0$ the standard phase field energy functional E approaches to the discrete brittle fracture energy functional in the sense of Γ -Convergence [2]. This implies increasingly smaller values of ϵ should be chosen, which is ultimately computationally expensive. To circumvent this issue, we interpret ϵ as a field variable, consequently argument of the energy function E . Furthermore, a regularization term $\beta\epsilon$ is added to the energy functional of the standard phase field model resulting in

$$E(\mathbf{u}, c, \epsilon) = \int_{\Omega} [1 - c]^2 \psi(\boldsymbol{\epsilon}) + \mathcal{G}_c \left[\frac{c^2 + \eta}{2\epsilon} + \frac{\epsilon}{2} |\nabla c|^2 \right] + \beta\epsilon \mathbf{d}x \quad (2)$$

now ϵ is spatially varying variable, and β and η are a penalty and model parameter respectively. Minimizing the energy functional (2) with respect to \mathbf{u} , c and ϵ we obtain the following Euler-Lagrange equations

$$\begin{aligned} \nabla \cdot \boldsymbol{\sigma} &= \mathbf{0} \quad \text{in } \Omega \\ \frac{c\mathcal{G}_c}{\epsilon} - 2[1 - c]\psi(\boldsymbol{\epsilon}) - \mathcal{G}_c \nabla \cdot [\epsilon \nabla c] &= 0 \quad \text{in } \Omega \\ \epsilon &= \sqrt{\frac{c^2 + \eta}{|\nabla c|^2 + \frac{2\beta}{\mathcal{G}_c}}} \quad \text{in } \Omega \end{aligned} \quad (3)$$

In addition to these equations of motion (3), the typical boundary conditions for phase-field problems are $\mathbf{u} = \mathbf{u}_0$ on $\partial\Omega_d$, $c = c_0$ on $\partial\Omega_p$ and $\nabla c \cdot \mathbf{n} = 0$ on $\partial\Omega \setminus \partial\Omega_p$. As these are nonlinear PDEs the choice of η and β is not straight forward and very sensitive. It is chosen such that the ϵ is smaller at the crack-tip or in the region of larger stress and large everywhere else. The domain is discretized using linear and quadratic finite elements for \mathbf{u} and c respectively. The discrete problem is solved using a staggered approach. We have implemented this for a Single Edge Notch Tension (SENT) specimen as seen in Figure 1 for $\eta = 421.87$ and $\beta = 3.125$.

¹Division of Engineering and Applied Sciences, California Institute of Technology, California, USA

²Lehrstuhl für Festkörpermechanik, Universität Siegen, 57076 Siegen, Germany

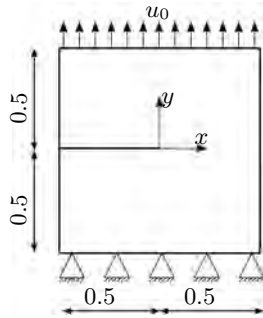


Figure 1: 2D problem set-up

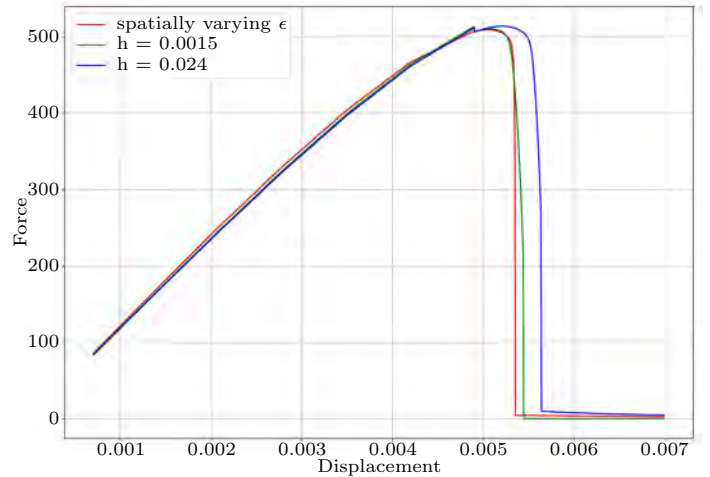
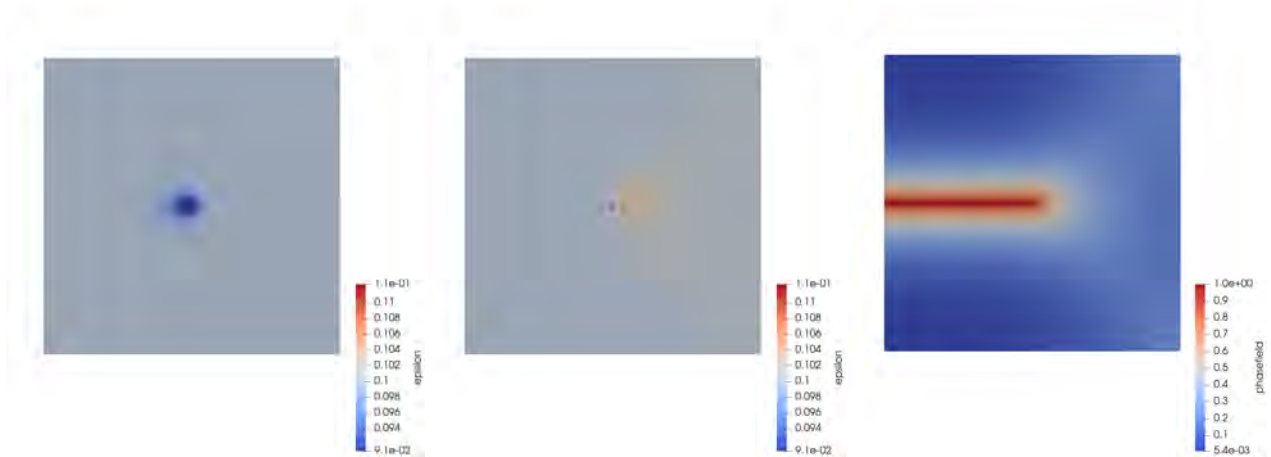


Figure 2: Force vs displacement plot

Figure 3: Evolution of ϵ with displacement $u_0^y = 0.0007, 0.005047$ and phase field at $u_0^y = 0.005047$

The force vs displacement plots are largely comparable with that of the standard phase field model of constant $\epsilon = 0.1$ as in the Figure 2. Evolution of ϵ w.r.t. displacement can be seen in Figure 3 and it illustrates ϵ is indeed smaller at the crack tip. The next step is to develop robust mesh refinement strategy utilizing this spatially varying ϵ .

Acknowledgement : The German Research Foundation (DFG) is gratefully acknowledged for funding this research within the research training group GRK2423 FRASCAL.

References

- [1] T. Gerasimov and L. de Lorenzis. *A Line Search Assisted Monolithic Approach for Phase-Field Computing of Brittle Fracture*. Computer Methods in Applied Mechanics and Engineering, 312:276-303, 2016.
- [2] A. Giacomini. *Approximation of Quasi-Static Evolution of Brittle Fractures*. Calculus of Variations and Partial Differential Equations, 22:129-172, 2005.

Grasping via kinematically reduced model of the hand

Uday Phutane, Michael Roller¹, and Sigrid Leyendecker

The hand is a complex end-effector to model as a multibody system due to its 20 degrees of freedom for the 15 joints. However, coordination has been observed between the fingers due to the underlying muscle-tendon structure [1]. In the director formulation for multibody dynamics, see [2], to move the hand from time node n to $n + 1$ local reparameterisation $\mathbf{q}_{n+1} = \mathbf{F}(\mathbf{u}_{n+1}, \mathbf{q}_n)$ is performed, where $\mathbf{q}_{n+1} \in \mathbb{R}^{288}$ and \mathbf{q}_n are configurations at time nodes $n + 1$ and n , respectively, and $\mathbf{u}_{n+1} \in \mathbb{R}^{26}$ is the discrete kinematic update. The coordination between fingers can be expressed through a synergy matrix $\mathbf{S} \in \mathbb{R}^{20 \times 15}$, which has been determined through experiments performed in [1]. By defining a synergy vector $\mathbf{z}_{n+1} \in \mathbb{R}^{n_z}$, where n_z is the number of synergies, the joint angle update can be calculated for 20 joints using anywhere between 1 to 15 synergies, through $\mathbf{u}_{n+1} = \mathbf{S}\mathbf{z}_{n+1}$. The local reparameterisation therefore reads as $\mathbf{q}_{n+1} = \mathbf{F}_d(\mathbf{S}\mathbf{z}_{n+1}, \mathbf{q}_n)$. The grasping is performed by solving an optimisation problem to minimise $J = J_1 + J_2$. J_1 minimises the distance between the finger and the object, while J_2 minimises the penetration between finger and object by maximising the tangential contact between finger and object surfaces, see details and equations in [3]. Here, we present two



Figure 1: The final postures for grasping a cylinder (left) and a sphere (right) with 3 contact points. The hand is kinematically actuated through 5 synergies which control the 20 joint angles.

grasps with a cylinder and a sphere, each performed with a single contact point on two fingers and a thumb, as shown in Figure 1. In each grasp, the objective values at the final positions are $3.32e^{-12}$ and $7.85e^{-11}$ for the cylinder and sphere, respectively. Furthermore, an objective value of $1.49e^{-11}$ was obtained for grasping the sphere with only 3 synergies, showing the flexibility and the scope of order reduction, thus saving computational costs.

References

- [1] M. Santello, M. Flanders and J.F. Soechting (1998). Postural hand synergies for tool use. *Journal of neuroscience*, 18(23), 10105-10115.
- [2] S. Leyendecker, S. Ober-Blöbaum, J.E. Marsden, and M. Ortiz (2010). Discrete mechanics and optimal control for constrained systems. *Optimal Control Applications and Methods*, 31(505-528).
- [3] U. Phutane, M. Roller, A. Boebel and S. Leyendecker (2020). Optimal Control of Grasping Problem Using Postural Synergies. In *Proceedings of the 6th International Digital Human Modeling Symposium* (pp. 206-213), Skövde, SE.

¹Fraunhofer Institute for Industrial Mathematics, Kaiserslautern, Germany

Understanding variational integrators in field theories

Rodrigo T. Sato Martín de Almagro, Sigrid Leyendecker

Geometric integration involves the numerical solution of differential equations using generic or specific methods that intend to preserve some or all features or underlying structures that the original problem displays.

One particular branch of geometric integration methods that our chair is interested in is variational methods [1, 2], which are already an important tool in the simulation of mechanical systems. These are methods whose main domain of application encompasses all systems whose behaviour can be derived from a variational principle such as Hamilton's principle of stationary action, as well as systems related to these but whose behaviour is not purely variational.

Such systems display important qualitative features that should ideally be present in the results of a simulation, such as conservation of quantities due to symmetries in the system (Noether's theorem) or compliance with specified constraints.

Variational methods are already being applied in the study and simulation of standard mechanical systems such as systems of massive particles and rigid bodies, as well as related optimal control problems, where the dynamics are governed by ordinary differential equations (ODEs). Another branch of application is on field theories, where the resulting equations are partial differential equations (PDEs). These include the equations of finite strain elasticity for non-dissipative materials, perfect fluids, electrodynamics and even those of general relativity.

The study and use of variational methods in this latter branch is still not as extended or as well-understood as in the former. In many cases, these are being coupled with standard spatial discretization techniques based on the finite element method, thus inheriting some of its strengths but also some of its problems. For that matter, we are trying to understand the basics of these methods while also trying to come up with better spatial discretization techniques.

Currently there are several problems we are researching:

- We are studying known multi-symplectic methods [3, 4] in the framework of variational integrators to better understand the properties and expected behaviour of these methods as well as obtain insight into the generation of more general methods. For this, we are mostly focusing on the 2D Poisson and 1D wave equations, which are some of the simplest variational models in PDEs, and serve as toy models for other systems such as the geometrically exact beam (fig. 1) and plate.

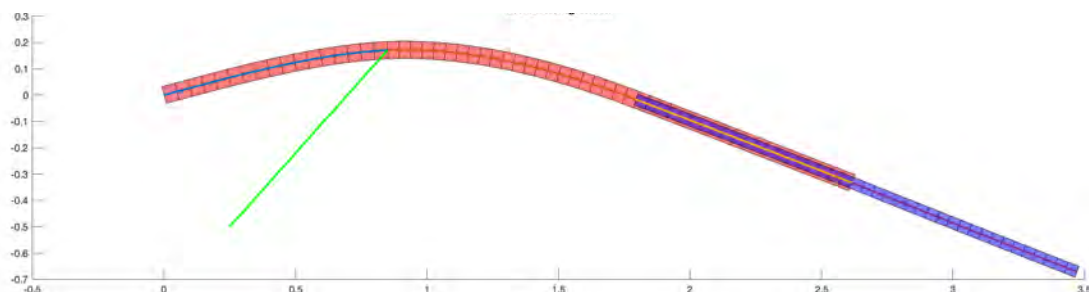


Figure 1: A 2D geometrically exact beam with variable sections modelling a telescopic boom pinned on one end and with an extendible support. This is an example of a constrained field theory on a Lie group. Its flexibility has been exaggerated.

- We are studying high order collocation-based numerical integration methods in triangular meshes. Collocation methods on unstructured meshes of triangular elements (fig. 2) do not seem to have been well-explored in the literature in favour of easier to implement and understand Galerkin methods. However, collocation methods are devoid of certain numerical artifacts that Galerkin methods can display [5], they can give us sharper accuracy estimates and have interesting consequences as to the interpretation of the discrete version of a theory.

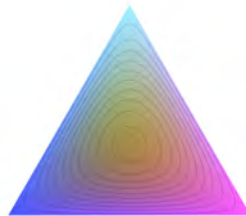


Figure 2: Single element 10-point Lobatto integration of the Poisson equation with unit source term in an equilateral triangle. The method is exact for general polynomials in 2 variables of order 3 and the solution of the problem turns out to be one such polynomial, so the integration is exact.

- Finally, in the standard mechanical front, we are also interested in extending the construction of collocation nonholonomic methods in [6, 7] to Galerkin methods. This might lead to easier construction of nonholonomic integrators.

References

- [1] Jerrold E. Marsden and Matthew West. Discrete mechanics and variational integrators. *Acta Numerica*, 10:357-514, 2001.
- [2] Ernst Hairer, Christian Lubich, and Gerhard Wanner. Geometric numerical integration: structurepreserving algorithms for ordinary differential equations. *Springer series in computational mathematics*. Springer, Berlin, Heidelberg, New York, 2006.
- [3] Thomas J. Bridges and Sebastian Reich. Multi-symplectic integrators: numerical schemes for Hamiltonian PDEs that conserve symplecticity. *Phys. Lett. A*, 284(4-5):184-193, 2001.
- [4] Robert I. McLachlan, Brett N. Ryland, and Yajuan Sun. High order multisymplectic Runge-Kutta methods. *SIAM J. Sci. Comput.*, 36(5):A2199-A2226, 2014.
- [5] Thomas Leitz, Rodrigo T. Sato Martín de Almagro, and Sigrid Leyendecker. Multisymplectic galerkin Lie group variational integrators for geometrically exact beam dynamics based on unit dual quaternion interpolation – no shear locking. *Computer Methods in Applied Mechanics and Engineering*, 374:113475, 2021.
- [6] R. T. Sato Martín de Almagro. Convergence of Lobatto-type Runge-Kutta methods for partitioned differential-algebraic systems of index 2. (*preprint, arXiv:1810.10298*). Submitted, 10, 2018.
- [7] D. Martín de Diego and R. T. Sato Martín de Almagro. High-order geometric methods for non-holonomic mechanical systems. (*preprint, arXiv:1810.109 26*). Submitted, 10, 2018.

Forward dynamics simulation of a human leg with a carbon spring prosthetic foot

Eduard S. Scheiterer, Sigrid Leyendecker

To accurately simulate a given system, it is necessary for the model to represent the key aspects of the system. These, of course, depend on the goal of the simulation and the available computing power. In case of the human leg with a prosthetic foot during gait, the model has to represent the movement of the different body parts while also capturing the deformation energy stored in the prosthetic foot. In this work, thigh and shank are modelled as rigid bodies in the director formulation, see [3], while the prosthetic foot is modelled as a predeformed geometrically exact beam, as seen in [1]. This allows for analysis of the simulation results with respect to joint angles, segment positions as well as the energy storage characteristics of the prosthetic foot. While the first two are obviously relevant to human gait, the storage and release of energy in the prosthetic foot during gait is considered a key aspect in prosthetic foot design, since it has a direct effect on the walking comfort of the patient.

The leg is modelled as a kinematic chain, i.e. a series of rigid bodies and flexible bodies connected by joints. The hip is modelled as a spherical joint between the thigh and reference frame. The knee joint is reduced to a single degree of freedom, the rotation about one axis, and is thus modelled as a revolute joint and not as a sliding hinge joint. The prosthetic foot is rigidly attached to the shank, mimicking a passive prosthetic foot. This means that there is no actuator inputting energy into the prosthetic foot during gait. In this work parameters based on [2] are used for mass, inertia and size, while the prosthetic foot is modelled after the Össur Vari-Flex[®] carbon spring prosthesis. Internal constraints ensure the rigidity of the segments, while the joints and rigid attachment are enforced via external constraints, shown in the following equations and explained in more detail in [3].

$$\begin{aligned} \mathbf{g}_{\text{sph}}(\mathbf{q}) &= \boldsymbol{\varphi}^1 - \boldsymbol{\varphi}^{\text{hip}} + \boldsymbol{\varrho}^1 = \mathbf{0} \\ \mathbf{g}_{\text{rev}}(\mathbf{q}) &= \begin{bmatrix} \boldsymbol{\varphi}^2 - \boldsymbol{\varphi}^1 + \boldsymbol{\varrho}^2 - \boldsymbol{\varrho}^1 \\ (\mathbf{n})^T \cdot \mathbf{d}_1^2 - \eta_1 \\ (\mathbf{n})^T \cdot \mathbf{d}_2^2 - \eta_2 \end{bmatrix} = \mathbf{0} \\ \mathbf{g}_{\text{rig}}(\mathbf{q}) &= \begin{bmatrix} \boldsymbol{\varphi}^3 - \boldsymbol{\varphi}^2 + \boldsymbol{\varrho}^3 - \boldsymbol{\varrho}^2 \\ \mathbf{d}_1^3 \cdot \mathbf{d}_2^2 - \eta_3 \\ \mathbf{d}_2^3 \cdot \mathbf{d}_3^2 - \eta_4 \\ \mathbf{d}_3^3 \cdot \mathbf{d}_1^2 - \eta_5 \end{bmatrix} = \mathbf{0} \end{aligned}$$

Here, \mathbf{q}^j denotes the j -th segments configuration, consisting of the centre of mass location $\boldsymbol{\varphi}^j$ and the directors \mathbf{d}_i^j , with $i \in 1, 2, 3$. η_k compensates for initial configurations of the constraints, while $\boldsymbol{\varrho}^j$ offsets the joint location from the centre of mass of body j . The prosthesis' deformation energy is modelled with a St. Venant-Kirchhoff-type stored energy function which describes an ideally elastic material behaviour, similar to Hook's law for simple elastic material.

$$W_{\text{int}}(\boldsymbol{\Gamma}, \mathbf{K}) = \frac{1}{2} \boldsymbol{\Gamma}^T \cdot \mathbf{D}^\Gamma \cdot \boldsymbol{\Gamma} + \frac{1}{2} \mathbf{K}^T \cdot \mathbf{D}^K \cdot \mathbf{K}.$$

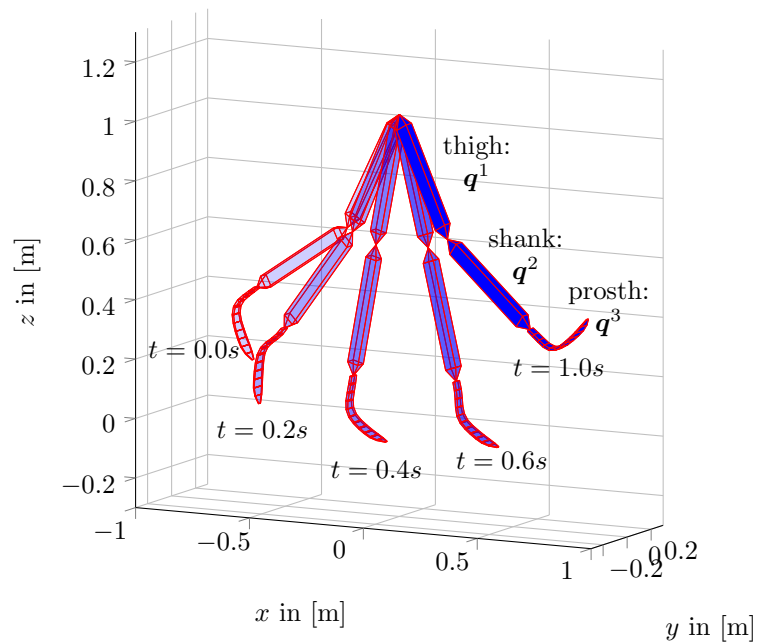


Figure 1: Simulation result of the swing movement for the human leg with a predeformed geometrically exact beam model for the prosthetic foot.

The material specific parameter matrices $\mathbf{D}^\Gamma = \text{diag}(GA, GA, EA)$ and $\mathbf{D}^K = \text{diag}(EI_1, EI_2, GJ)$ consist of the Young's modulus E , the shear modulus G and geometry specific parameters e.g. the cross-section area A , the area moments of inertia I_1, I_2 and the polar moment of inertia J . The strain measures $\mathbf{\Gamma}(\mathbf{q})$ and $\mathbf{K}(\mathbf{q})$ quantify shear, elongation, flexion and torsion.

In this simulation the model is subject to a gravitational field and no forces or moments are applied to the system. In its initial state at $t = 0.0\text{s}$ the system is at rest and the prosthesis is not deformed. Figure 1 visualises the model and the results of the forward dynamics simulation, while Figure 2 shows the energy evolution over time for multiple oscillations. The simulation shows a swinging motion of the human leg with prosthetic foot, mimicking the swing phase of the human gait cycle. The Young's modulus of the prosthesis is reduced compared to carbon fibre laminate, in order to emphasise its deformation. A variational integrator is used to solve the resulting set of equations, derived from the discrete action principle for the discretised augmented Lagrangian, see [3]. As can be seen in Figure 2 the energy is exchanged between the potential, kinetic and internal deformation energy. It is important to note, that due to the variational integrator, which is structure preserving, the total energy of the system is bounded for the entire simulation.

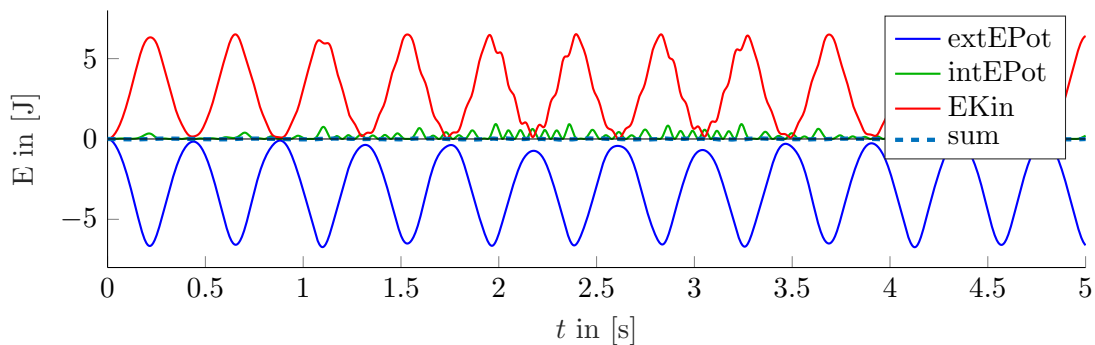


Figure 2: Evolution of the different energy components over time for the pendulum simulation.

With the forward dynamics simulation of the human leg successfully implemented, the next step is to create different configurations and constraint settings that emulate phases occurring during natural gait. Furthermore, it is possible to apply fuzzy forward dynamics to the model, via the graph follower algorithm from [4]. For this, the main question is, what sensible target outputs are with respect to human gait.

Acknowledgements

The support of this work by the German Research Foundation (DFG) through the priority program SPP1886 is gratefully acknowledged.

References

- [1] S. S. Antman, *Nonlinear Problems of Elasticity*. Springer, 1995.
- [2] Chandler, R. F. et al: *Investigation of inertial properties of the human body*. Air Force Aerospace Medical Research Lab Wright-Patterson AFB OH, 1975
- [3] Leyendecker, S.; Marsden, J.E.; Ortiz, M.: *Variational integrators for constrained dynamical systems*. ZAMM-Journal of Applied Mathematics and Mechanics, Vol. 88, p. 677-708, 2008.
- [4] Eisentraudt, M. and Leyendecker, S.: *Fuzzy uncertainty in forward dynamics simulation*. Mechanical Systems and Signal Processing, 2019

Variational integrators used to solve a 1D wave equation

Martina Stavole, Sigrid Leyendecker



Variational integrators for mechanical systems are derived by discretizing Hamilton's principle of stationary action [1]. The variational derivation of the integrators guarantees some favourable properties such as good energy behaviour meaning the energy error does not increase or decrease over simulation time but stays bounded. If there are symmetries in the mechanical system (Noether's theorem), variational integrators conserve the corresponding momentum maps. As an example, it is shown here a variational formulation of the 1D wave equation which is a second-order linear PDE and it is used to model small oscillation around the equilibrium. In the continuous case, the Lagrangian of the system reads

$$L(u, \dot{u}, u') = T(\dot{u}) - U(u') = \frac{1}{2}\rho\dot{u}^2 - \frac{1}{2}ku'^2$$

where T is the kinetic energy, U is the potential energy, ρ is the string density per unit length, k is the stiffness. The local coordinate is u , $\dot{u} = \frac{\partial u}{\partial t}$, $u' = \frac{\partial u}{\partial x}$, where t denotes the time and x the space. Applying Hamilton's principle yields the Euler-Lagrange equation.

In the discrete case, the trapezoidal quadrature rule is used to approximate the integral of the Lagrangian. For the space-time integration, a discretization is defined in both time and space, where Δt and Δx are respectively the time step size and the space step size. The discrete Lagrangian is an approximation of the continuous action for one space time element, see Figure 1.a, reading

$$L_d^{i,j}(u_{i,j}, u_{i+1,j}, u_{i,j+1}, u_{i+1,j+1}) \approx \int_{x_i}^{x_{i+1}} \int_{t_j}^{t_{j+1}} L(x, t, u, \dot{u}, u') dt dx$$

The discrete variational principle yields the discrete Euler-Lagrange equations. In order to uniquely solve the dynamics of the problem, initial and boundary conditions are needed. In the post-processing the discrete conjugate momenta are calculated by the discrete Legendre transforms. Figure 1.b shows the simulated energy density evolution. The wave equation is just a simple variational model in PDEs studied in order to move to more complex systems like the geometrically exact beam in the future.

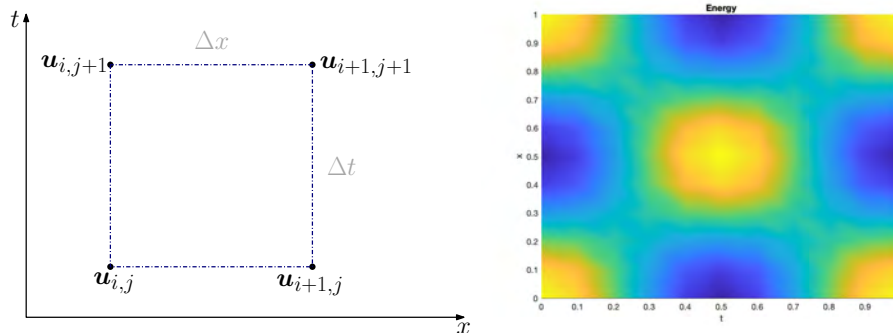


Figure 1: a.Space time grid, b.Energy density evolution

References

- [1] J.E. Marsden and M. West, Discrete mechanics and variational integrators, Acta Numerica (2001)

Analysis of multirate variational integrators and mixed order variational integrators by Modulated Fourier expansions

Theresa Wenger, Sina Ober-Blöbaum, Sigrid Leyendecker

The simulation of mechanical systems that act on multiple time scales is challenging. For resolving the fast motion a tiny time step is required, whereas for the slow motion a coarser approximation is accurate enough, pointing out the conflict of highly accurate results versus low computational costs. The presented integrators are designed to efficiently solve such multirate systems.

The derivation of the multirate variational integrators and the mixed order variational integrators bases on a discrete version of Hamilton's principle. The idea of the multirate approach is to split the variables into slow and fast ones enabling to approximate them on different time grids and to use different quadrature rules with different time steps to approximate the contributions of the action. Whereas in the mixed order approach one time grid is used, but different polynomials are considered for the slow and fast degrees of freedom together with different quadrature rules of appropriate order for the contributions of the action. Due to their variational derivation, the integrators preserve the underlying geometric structure of the system as momentum maps and symplecticity.

We consider a highly oscillatory dynamical system with a Lagrangian of form

$$L(q^s, q^f, \dot{q}^s, \dot{q}^f) = \frac{1}{2} \dot{q}^T \dot{q} - V(q) - \frac{1}{2} \omega^2 (q^f)^2 \quad (1)$$

where $\omega \gg 1$. The configuration q is split in n^s slow variables q^s and n^f fast variables q^f . The slow potential V is assumed to be nonlinear. Systems of the form as given in (1) have some characteristics, what can be shown by the modulated Fourier expansion, see [HLW06]. A slow energy exchange between the oscillatory components takes place on the time scale ω . The energy stored in the j -th stiff component is $I_j = \frac{1}{2} (\dot{q}_j^f)^2 + \frac{1}{2} \omega^2 (q_j^f)^2$, $j = 1, \dots, n^f$. The total stiff energy $I = \sum_j I_j$ is an adiabatic invariant with $\mathcal{O}(\omega^{-1})$ deviations from the initial value over very long time intervals.

For the multirate approach we introduce a macro time grid $\{t_k = k\Delta T | k = 0, \dots, N\}$ with time step ΔT and a micro grid $\{t_k^m = k\Delta T + m\Delta t | k = 0, \dots, N-1, m = 0, \dots, p\}$ with time step $\Delta t = \frac{\Delta T}{p}$, $p \in \mathbb{N}$. For the mixed order approach one time grid, i.e. the macro time grid, is used. We focus on one special variant each, where the symmetric trapezoidal rule is used to approximate the integral of the slow potential on the macro grid. Both variants can be written in style of an impulse method with an explicit kick of the slow force, updating the fast oscillations implicitly, and an explicit kick of the slow force in the end. In the multirate framework the midpoint rule is used to update the fast oscillations on the micro grid. The mixed order approach uses a s -stage Gauss collocation method to approximately compute the fast oscillations. Both schemes can be interpreted as modified trigonometric integrators for a modified frequency $\tilde{\omega}$. The capture of the systems' characteristics by trigonometric integrators as well as modified trigonometric integrators is analysed by the tools of the modified Fourier expansion in [HLW06] and [MS14]. Following the analysis in [MS14] it can be shown that both considered schemes conserve the oscillatory and total energy up to $\mathcal{O}(\Delta T)$ and that they capture the energy exchange between the stiff components correctly.

The Fermi-Pasta-Ulam problem (FPU) is an example of a nontrivial highly oscillatory conservative system with a Lagrangian of form as given in (1). Due to its rich multiscale coupling behaviour, the FPU is a popular test problem for numerical integrators. It consists of 2ℓ masses linked with alternating weak cubic and stiff linear springs. The slow variables represent the location of the centre of the stiff springs and the fast variables are their lengths. In our simulations we include six masses, thus three stiff springs. Figure 1 and 2 (left plot) show the phenomenon of slow energy exchange between the stiff springs I_1, I_2, I_3 and the adiabatic invariant $I = I_1 + I_2 + I_3$. The evolution of the error in the total energy over time is shown in Figure 1 and 2 (right plot). Both, the mixed order and the multirate variational integrator, capture the stiff energy exchange. The plots further show that the total oscillatory energy I and the total energy are conserved up to $\mathcal{O}(\Delta T)$ with $\Delta T = 0.1$.

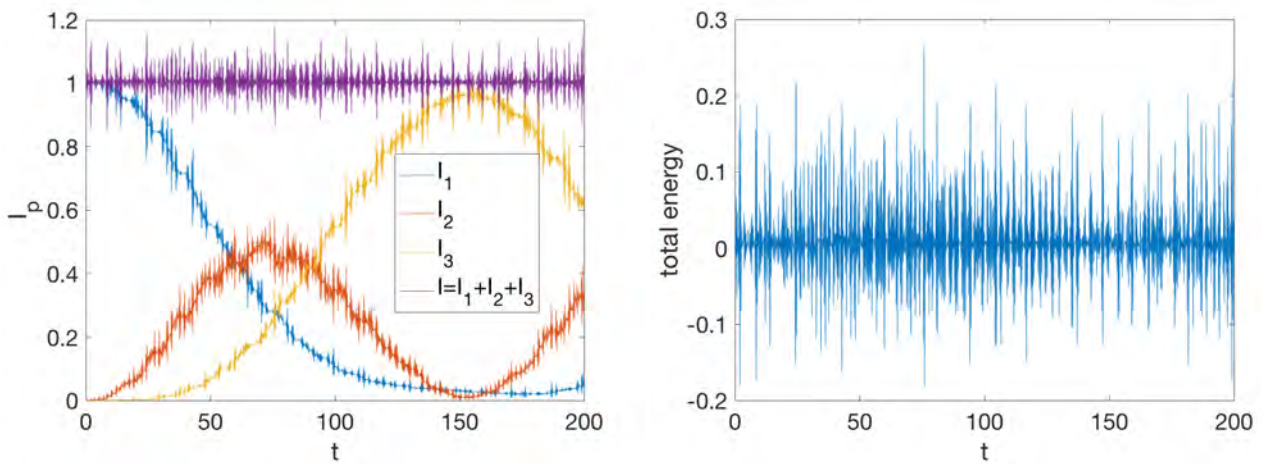


Figure 1: Mixed order variational integrator with $\Delta T = 0.1$, $s = 3$: energy in the stiff springs and total oscillatory energy (left), error in the total energy (right)

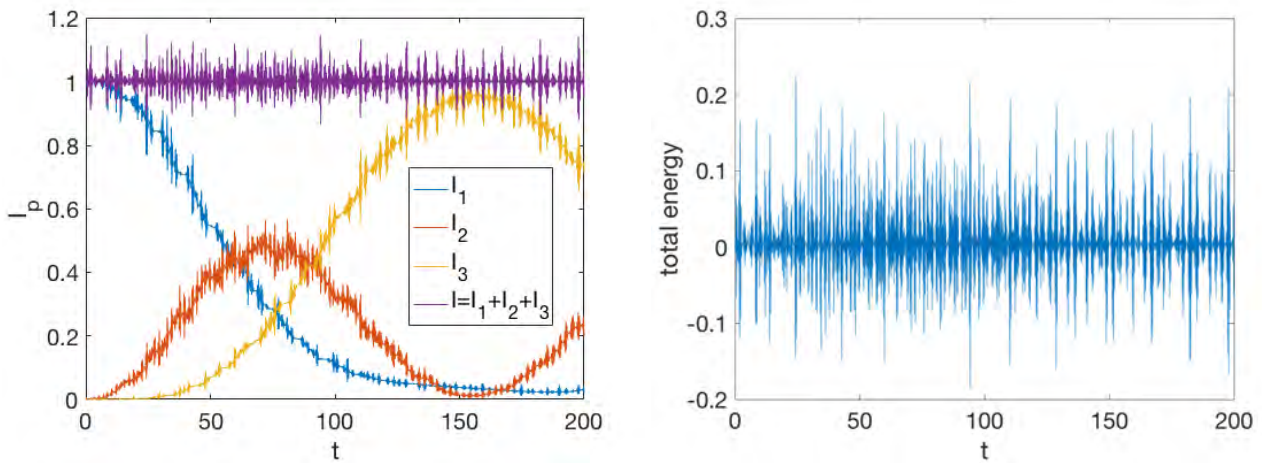


Figure 2: Multirate variational integrator with $\Delta T = 0.1$, $p = 5$: energy in the stiff springs and total oscillatory energy (left), error in the total energy (right)

References

- [HLW06] Ernst Hairer, Christian Lubich, and Gerhard Wanner. *Geometric numerical integration: structure-preserving algorithms for ordinary differential equations*, volume 31 of *Springer Series in Computational Mathematics*. Springer, Berlin Heidelberg, 2006.
- [MS14] R. McLachlan and A. Stern. Modified trigonometric integrators. *SIAM Journal on Numerical Analysis*, 52(3):1378–1397, 2014.

4 Activities

4.1 Teaching during Covid-19 pandemic

The year 2020 was distinct. The entire world has been facing a pandemic and had to adapt the old routine to a new normality. This meant strictly following measures such as social distancing and hygiene best practices. One of the most important measures that the Institute of Applied Dynamics followed and adapted this year was the digital teaching. Most of our lectures, excersices and tutorials were streamed live, recorded and uploaded via zoom, StudOn and other digital meeting platforms.

In the case of the matlab laboratory, the Maschinenbau CIP-Pool remained closed or in some cases remotely inaccessible to students. Tutors acted accordingly and adapted the course using a remote connection with the help of the 'Informatik CIP-Pool'. The students were able to perform the exercises remotely and receive feedback in digital form.

The dynamic practical course reduced the number of participants according with the university regulations, the course took place with students on site following strict hygiene measures and social distancing at all times. This implied, the students had to carry out the group activity of the experiments via zoom. To accomplish the general social distancing and hygiene measures, LTD re-organised and adequated the rooms with projectors, flexi-glas curtains and sanitation supplies.



Exams revisions 12.2020

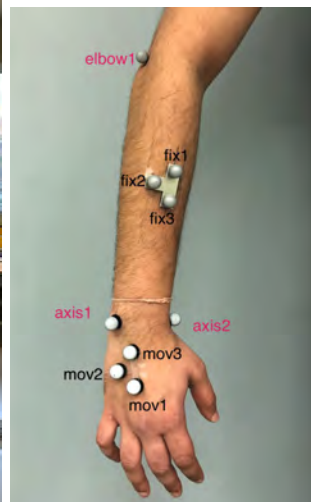




4.2 Motion capture laboratory

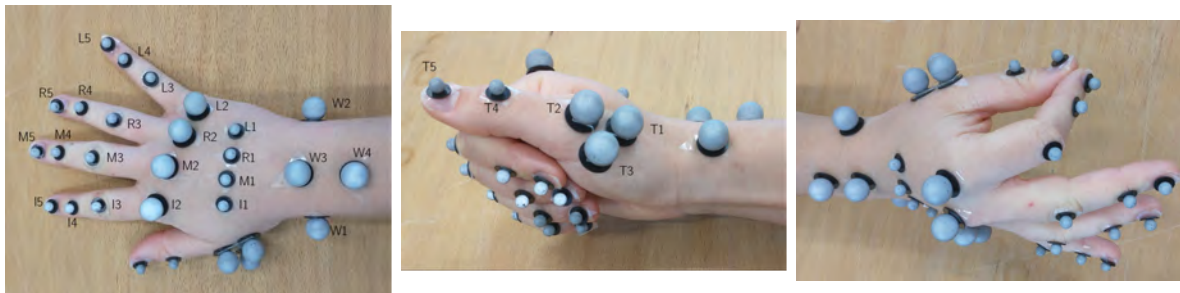
Our motion analysis lab is equipped with a camera and marker based optical tracking system. This includes 10 Qualisys MoCap high speed cameras and 2 Qualisys high speed video cameras, Noraxon MyoMotion inertial sensors, Cybergloves III to measure hand joint angle kinematics, force plates, and Noraxon Desktop DTS electromyography sensors.

A frame was constructed to bring the cameras closer to the markers in order to perform motion capturing for small human actions, such as motion of hand digits. With this setup, kinematic parameter identification for joints in the human hand, especially the wrist, the metacarpophalangeal and interpalangeal joints has been performed. This is an essential first step towards formulating a procedure for effective parameter identification to setup subject-specific models. This will enable us to perform biomechanical optimal control simulations with higher levels of confidence and use the results as measures of human performance.



The motion capture laboratory increased its performance by taking a step forward with the measurement of

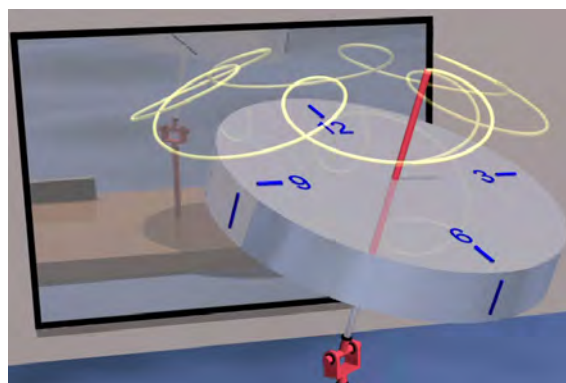
patients in cooperation with the Department of Medicine 3 - Rheumatology and Immunology of the Universitätsklinikum Erlangen. One of this year measurementnets developed a SBF proposal; the test consisted of two measurements without motion capturing equipment and a few more with equipment.



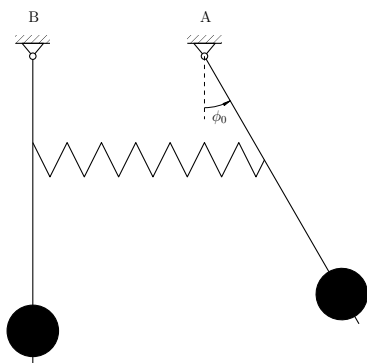
4.3 Dynamic laboratory

The dynamic laboratory – modeling, simulation and experiment (Praktikum Technische Dynamik) addresses all students of the Technical Faculty of the Friedrich-Alexander-Universität Erlangen-Nürnberg. The aim of the practical course is to develop mathematical models of fundamental dynamical systems to simulate them numerically and compare the results to measurements from the real mechanical system. Here, the students learn both the enormous possibilities of computer based modeling and its limitations. The course contains one central programming exercise and six experiments observing various physical phenomena along with corresponding numerical simulations:

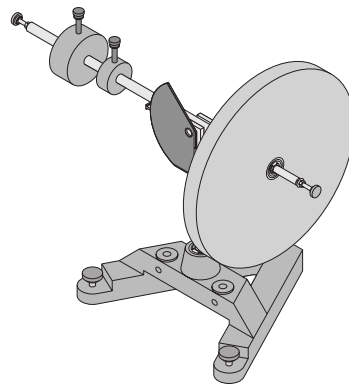
- programming training
- beating pendulums
- gyroscope
- ball balancer
- robot arm
- inverse pendulum
- balancing robot



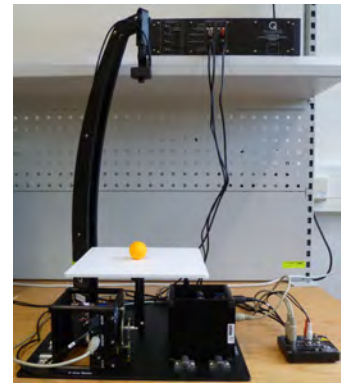
programming training



beating pendulums



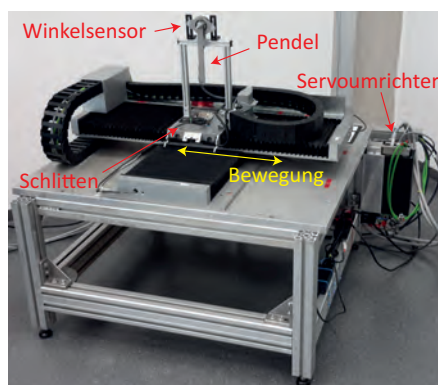
gyroscope



ball balancer



robot arm



inverse pendulum



balancing robot

4.4 MATLAB laboratory

The MATLAB laboratory (Praktikum MATLAB) is offered to all students of the Technical Faculty of the Friedrich-Alexander-Universität Erlangen-Nürnberg. The course aims to teach the participants the basic skills of mathematical programming in MATLAB. The course is offered in conjunction with the Chair of Applied Mechanics (LTM), the Chair of Production Metrology (FMT) and the Chair of Engineering Design (KTmfk). The first lecture is an introductory programming session for MATLAB fundamentals. Thereafter, every chair presents a task related to mechanics and engineering, for example, the LTD task is to understand and simulate, the dynamics of a crane. The task is introduced to the students through a theory lecture, which is then followed by programming sessions.

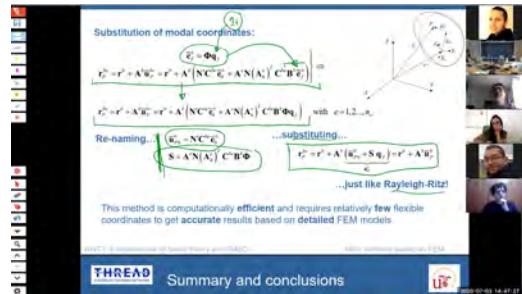
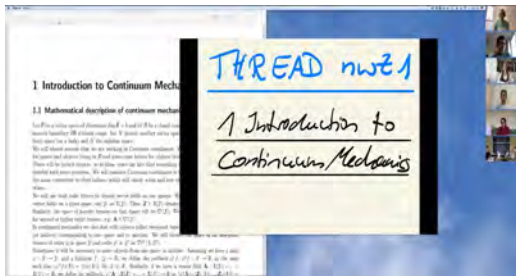
4.5 Summer school: Fundamentals of beam theory and flexible multibody dynamics

The summer school “Fundamentals of beam theory and flexible multibody dynamics”, was organised and conducted by the Institute of Applied Dynamics under the project “Numerical Modelling of Highly Flexible Structures for Industrial Applications (THREAD)”, from June 29th to July 3rd, 2020. The participants took part via zoom worldwide.

The main objective of this training event was to let the researchers reach common ground. For this, they were presented with classic and state-of-the-art models and analytic techniques used in describing beam-like structures subjected to small and large deformations and flexible multi-body systems under the assumption of small elastic deformations. An introduction to discretisation strategies and modal reduction was also part of the programme.

The summer school offered problem solving sessions for the participants where they were tasked to discuss and solve analytic and programming exercises in small groups and a guided resolution at the end of each session. The exercises were based on an industrial example provided by MEVEA.

As a result, throughout the course of the summer school the participants were able to interact with each other, in spite of the current conditions, integrating knowledge exchange with social interaction.



4.6 Teaching

Winter semester 2020/2021

Dynamik starrer Körper (MB, ME, WING, IP, BPT, CE, MT)

Vorlesung
Übung + Tutorium

S. Leyendecker
D. Holz, M. Klebl, H. Lang
D. Martonová, J. Penner
U. Phutane, T. Wenger

Mehrkörperdynamik (MB, ME, WING, TM, BPT, MT)

Vorlesung
Übung

S. Leyendecker
J. Penner

Geometric beam theory (MB, ME, WING, BPT)

Vorlesung + Übung

S. Leyendecker
R.T. Sato Martín de Almagro

Praktikum Technische Dynamik – Modellierung, Simulation und Experiment (MB, ME, WING)

S. Leyendecker
D. Holz, M. Klebl
D. Martonová, J. Penner
U. Phutane

Praktikum Matlab (MB)

S. Leyendecker
U. Phutane, E. Schaller
A. Müller, M. Franz

Summer semester 2020

Biomechanik (MT)

Vorlesung + Übung
geprüft 34 + 9 (WS 2019/2020)

S. Budday

Geometric numerical integration (MB, ME, WING, BPT)

Vorlesung

Übung
geprüft 4 + 0 (WS 2019/2020)

S. Leyendecker
R.T. Sato Martín de Almagro
E.S. Scheiterer

Statik und Festigkeitslehre (BPT, CE, ME, MWT, MT)

Vorlesung
Tutorium

Übung
geprüft 283 + 310 (WS 2019/2020)

S. Leyendecker
X. Chen, D. Holz, U. Phutane
M. Klebl, D. Martonová
X. Chen, D. Holz, M. Klebl

Praktikum Matlab (MB)			
Teilnehmer	56		S. Leyendecker U. Phutane, E. Schaller M. Franz, A. Müller
Fundamentals of beam theory and flexible multibody dynamics (THREAD)			
Vorlesung + Übung			R.T. Sato Martín de Almagro
Teilnehmer	45		S. Leyendecker
Winter semester 2019/2020			
Biomechanik der Bewegung (MT)			
Vorlesung + Übung			H. Lang
geprüft	15		
Dynamik starrer Körper (MB, ME, WING, IP, BPT, CE, MT)			
Vorlesung			S. Leyendecker
Tutorium			D. Holz, M. Klebl D. Martonová, U. Phutane
Übung			R.T. Sato Martín de Almagro D. Holz, M. Klebl U. Phutane
geprüft	248 + 124 (SS 2020)		
Mehrkörperdynamik (MB, ME, WING, TM, BPT, MT)			
Vorlesung			S. Leyendecker
Übung			J. Penner
geprüft	46 + 21 (SS 2020)		
Praktikum Technische Dynamik – Modellierung, Simulation und Experiment (MB, ME, WING)			
Teilnehmer	12		S. Leyendecker X. Chen, D. Holz, M. Klebl H. Lang, D. Martonová J. Penner, D. Phansalkar U. Phutane, R.T. Sato E.S. Scheiterer
Praktikum Matlab (MB)			
Teilnehmer	56		S. Leyendecker, U. Phutane Ö. Akar, A. Müller, M. Franz
Additional exams			
Hochschulpraktikum (M. Sc. Medizintechnik)			
geprüft	1		

4.7 Theses

Master theses

- Fabian Bengl
Variational integration of the Liouville equation: Numerical experiment
- Emely Schaller
Modelling the human heart – Comparison of MRI and simulation based cardiac motion
- Tianhui Zhang
Determination of kinematic parameters through motion capturing of human hand

Project theses

- Matthias Schubert
Control of an electromechanically coupled pendulum with MPC and DMOC

Bachelor theses

- Yousif Aljammal
Gelenkwinkelbestimmung beim menschlichen Gang aus optischem Tracking – Ein Vergleich

4.8 Seminar for mechanics

together with the Chair of Applied Mechanics LTM

- 09.12.2020 B.Sc. Julian Shanbag
Friedrich-Alexander-Universität Erlangen-Nürnberg
Entwicklung und Validierung eines Mehrkörper-Fußmodells zur Funktionsanalyse (juveniler) Fußdeformitäten
- 10.11.2020 Prof. Dr. Michael Ortiz
California Institute of Technology, Pasadena, CA
Multiscale modeling of ductile fracture in metals
- 03.02.2020 Jun.-Prof. Dr.-Ing. Malte Krack
Institut für Luftfahrtantriebe, Universität Stuttgart
Intentional Use of Nonlinearity for Passive Vibration Mitigation
- 22.01.2020 Prof. Dr. Anne Koelewijn
Machine Learning and Data Analytics Lab
Friedrich-Alexander-Universität Erlangen-Nürnberg
Predictive Movement Simulations – Finding the Holy Grail of Biomechanics

4.9 Editorial activities

Advisory and editorial board memberships Since January 2014, Prof. Dr.-Ing. habil. Sigrid Leyendecker is a member of the advisory board of the scientific journal *Multibody System Dynamics*, Springer. She is a member of the Editorial Board of *ZAMM – Journal of Applied Mathematics and Mechanics / Zeitschrift für Angewandte Mathematik und Mechanik* since January 2016 and since 2017 runs a second term as member of the managing board of the International Association of Applied Mathematics and Mechanics (GAMM), as well as a member of the executive council of the German Association for Computational Mechanics (GACM) and member of the General Council of the International Association for Computational Mechanics (IACM).

Since October 2017, Prof. Dr.-Ing. habil. Sigrid Leyendecker is an elected member of the Faculty Council of the Faculty of Engineering at the Friedrich-Alexander-Universität Erlangen-Nürnberg, and in April 2019 was elected deputy Chair of the Qualification Assessment Committee (Eignungsfeststellungsverfahrens-(EFV-)Kommission) of the Bachelor's degree programme Medical Engineering, at the Friedrich-Alexander-Universität Erlangen-Nürnberg.

5 Publications

5.1 Reviewed journal publications

1. D. Martonová, D. Holz, M.T. Duong and S. Leyendecker. “Towards the simulation of active cardiac mechanics using a smoothed finite element method”. *Journal of Biomechanics*, 2020 (accepted).
2. T. Leitz, R.T. Sato Martín de Almagro and S. Leyendecker. “Multisymplectic Galerkin Lie group variational integrators for geometrically exact beam dynamics based on unit dual quaternion interpolation – no shear locking”. *Computer Methods in Applied Mechanics and Engineering*, 2020 (accepted).

5.2 Invited lectures

1. S. Leyendecker. *Geometric numerical integration in simulation and optimal control – and other topics*. Annual Meeting 2020 – Joint Training on Numerical Modelling of Highly Flexible Structures THREAD, Kaiserslautern, Germany (Microsoft Teams), 19 -23 October 2020.

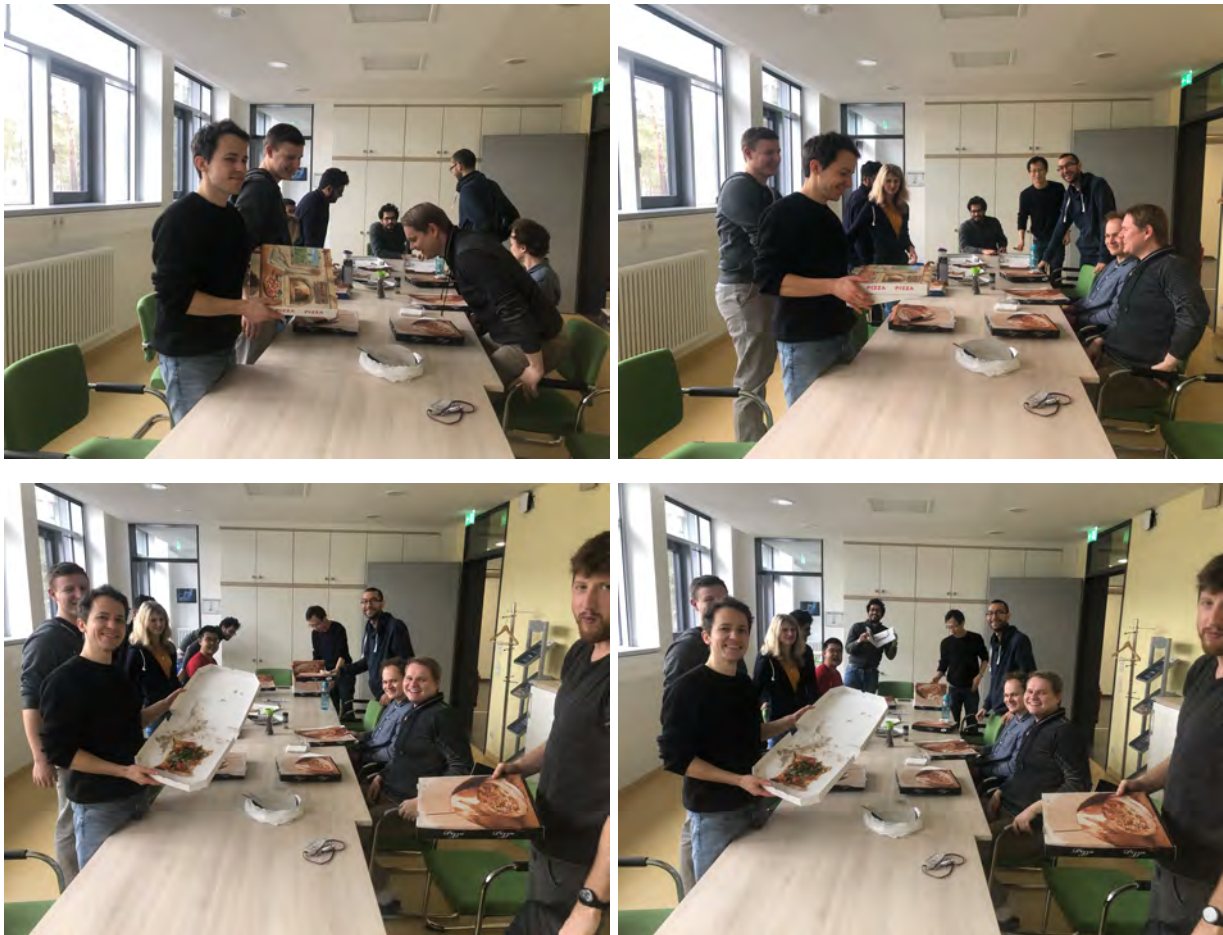
5.3 Conferences and proceedings

1. E.S. Scheiterer and S. Leyendecker. “Predeformed geometrically exact beam model for a dynamic-response prosthesis”. In: *Proc. Appl. Math. Mech.,PAMM*, DOI:10.1002/pamm.202000152, 2020 (accepted).
2. X. Chen, S. Leyendecker and H. van den Bedem. “Kinematic Flexibility Analysis of Active and Inactive Kinase Conformations”. In: *Proc. Appl. Math. Mech.,PAMM*, DOI:10.1002/pamm.202000166, 2020 (accepted).
3. Y. Lishkova, S. Ober-Blöbaum, M. Cannon and S. Leyendecker. “A multirate variational approach to simulation and optimal control for flexible spacecraft”. In: *Proceedings of the 2020 AAS/AIAA Astrodynamics Specialist Conference*, Lake Tahoe, 2020.
4. U. Phutane, M. Roller, A. Boebel and S. Leyendecker. “Optimal Control of Grasping Problem Using Postural Synergies”. In: *Proceedings of the 6th International Digital Human Modeling Symposium*, Skövde, Sweden, 2020.
5. J. Penner and S. Leyendecker. “Defining Kinematic Chains for Musculoskeletal Optimal Control Simulations via Automatic Differentiation”. In: *Proceedings of the 6th International Digital Human Modeling Symposium*, Skövde, Sweden, 2020.
6. M. Lohmayer and S. Leyendecker. ”Exergetic Port-Hamiltonian Systems – a tutorial”. *Student Compact Course – Variational Methods for Fluids and Solids*. Berlin, Germany (ZOOM), 12-23 October, 2020.
7. D. Huang and S. Leyendecker. ”On computational aspects of electromechanical coupling in geometrically exact beams dynamics”. *2020 Online Symposium on flexible multibody systems dynamics*. September 2020.
8. D. Phansalkar and S. Leyendecker. “On numerical challenges with a phase-field model for a mode I fracture”. *7th GAMM workshop on phase-field modeling*. Kaiserslautern, Germany, 10-11 February 2020.

6 Social events

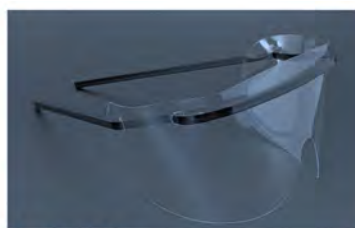
In 2020 most of the social activities were canceled due to the Covid-19 pandemic. Various hygiene measures were established, as well as social distancing from the second quarter of the year.

Lunch after a succesful presentation at LTD 02.2020

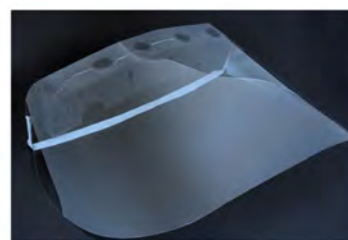


Volunteering during lockdown

During the last weeks of March, the Institute for Polymer Technology (LKT) started the production of protective equipment for the medical staff at Erlangen University Hospital. Our colleague Johann Penner, volunteered to help in the manufacture of protective goggles and visieren for this important social cause.



Montierte Brille,
(Foto: Marion Untheim, LKT)



Montiertes Visier,
(Foto: Marion Untheim, LKT)

Saint Nicholas visits LTD 07.12.2020

